












# Atrial fibrillation-associated electrical remodelling in human induced pluripotent stem cell-derived atrial cardiomyocytes: a novel pathway for antiarrhythmic therapy development

Fitzwilliam Seibertz <sup>1,2,3†</sup>, Tony Rubio <sup>1,2†</sup>, Robin Springer <sup>1,2†</sup>, Fiona Popp <sup>1,2</sup>, Melanie Ritter <sup>1,2</sup>, Aiste Liutkute <sup>1,2</sup>, Lena Bartelt <sup>1,2</sup>, Lea Stelzer <sup>1,2</sup>, Fereshteh Haghighi <sup>2,4</sup>, Jan Pietras <sup>2,4</sup>, Hendrik Windel <sup>2,4</sup>, Núria Díaz i Pedrosa <sup>1,2‡</sup>, Markus Rapedius <sup>5</sup>, Yannic Doering <sup>1,2</sup>, Richard Solano <sup>1,2,4</sup>, Robin Hindmarsh <sup>2,6</sup>, Runzhu Shi <sup>2,7</sup>, Malte Tiburcy <sup>1,2</sup>, Tobias Bruegmann <sup>2,3,7</sup>, Ingo Kutschka <sup>2,4</sup>, Katrin Streckfuss-Bömeke <sup>2,6,8</sup>, George Kensah <sup>2,4</sup>, Lukas Cyganek <sup>2,3,6</sup>, Wolfram H. Zimmermann <sup>1,2,3,9,10,11</sup>, and Niels Voigt <sup>1,2,3\*</sup>

<sup>1</sup>Institute of Pharmacology and Toxicology, University Medical Center Göttingen, Georg-August University Göttingen, Robert-Koch-Straße 40, 37075 Göttingen, Germany; <sup>2</sup>DZHK (German Center for Cardiovascular Research), partner site Göttingen, Germany; <sup>3</sup>Cluster of Excellence 'Multiscale Bioimaging: from Molecular Machines to Networks of Excitable Cells' (MBExC), University of Göttingen, Göttingen, Germany; <sup>4</sup>Department of Cardiothoracic and Vascular Surgery, Georg-August-University Göttingen, Göttingen, Germany; <sup>5</sup>Nanon Technologies GmbH, Munich, Germany; <sup>6</sup>Clinic for Cardiology and Pneumology, University Medical Center Göttingen, Georg-August University Göttingen, Germany; <sup>7</sup>Institute for Cardiovascular Physiology, University Medical Center Göttingen, Göttingen, Germany; <sup>8</sup>Institute of Pharmacology and Toxicology, University of Würzburg, Würzburg, Germany; <sup>9</sup>German Center for Neurodegenerative Diseases (DZNE), Göttingen, Germany; <sup>10</sup>Fraunhofer Institute for Translational Medicine and Pharmacology (ITMP), Göttingen, Germany; and <sup>11</sup>Campus-Institute Data Science (CIDAS), University of Göttingen, Göttingen, Germany

Received 28 September 2022; revised 18 July 2023; accepted 3 August 2023; online publish-ahead-of-print 7 September 2023

**Time of primary review: Days for primary review: days**

## Aims

Atrial fibrillation (AF) is associated with tachycardia-induced cellular electrophysiology alterations which promote AF chronification and treatment resistance. Development of novel antiarrhythmic therapies is hampered by the absence of scalable experimental human models that reflect AF-associated electrical remodelling. Therefore, we aimed to assess if AF-associated remodelling of cellular electrophysiology can be simulated in human atrial-like cardiomyocytes derived from induced pluripotent stem cells in the presence of retinoic acid (iPSC-aCM), and atrial-engineered human myocardium (aEHM) under short term (24 h) and chronic (7 days) tachypacing (TP).

## Methods and results

First, 24-h electrical pacing at 3 Hz was used to investigate whether AF-associated remodelling in iPSC-aCM and aEHM would ensue. Compared to controls (24 h, 1 Hz pacing) TP-stimulated iPSC-aCM presented classical hallmarks of AF-associated remodelling: (i) decreased L-type  $\text{Ca}^{2+}$  current ( $I_{\text{Ca,L}}$ ) and (ii) impaired activation of acetylcholine-activated inward-rectifier  $\text{K}^+$  current ( $I_{\text{K,ACh}}$ ). This resulted in action potential shortening and an absent response to the M-receptor agonist carbachol in both iPSC-aCM and aEHM subjected to TP. Accordingly, mRNA expression of the channel-subunit Kir3.4 was reduced. Selective  $I_{\text{K,ACh}}$  blockade with tertiapin reduced basal inward-rectifier  $\text{K}^+$  current only in iPSC-aCM subjected to TP, thereby unmasking an agonist-independent constitutively active  $I_{\text{K,ACh}}$ . To allow for long-term TP, we developed iPSC-aCM and aEHM expressing the light-gated ion-channel f-Chrimson. The same hallmarks of AF-associated remodelling were observed after optical-TP. In addition, continuous TP (7 days) led to (i) increased amplitude of inward-rectifier  $\text{K}^+$  current ( $I_{\text{K1}}$ ), (ii) hyperpolarization of the resting membrane potential, (iii) increased action potential-amplitude and upstroke velocity as well as (iv) reversibly impaired contractile function in aEHM.

\* Corresponding author. Tel: +00495513965174; fax: +00495513965169, E-mail: [niels.voigt@med.uni-goettingen.de](mailto:niels.voigt@med.uni-goettingen.de)

† The first three authors contributed equally to this study.

‡ Present address: Institute of Experimental Cardiology, Internal Medicine VIII, Heidelberg University, Heidelberg, Germany.

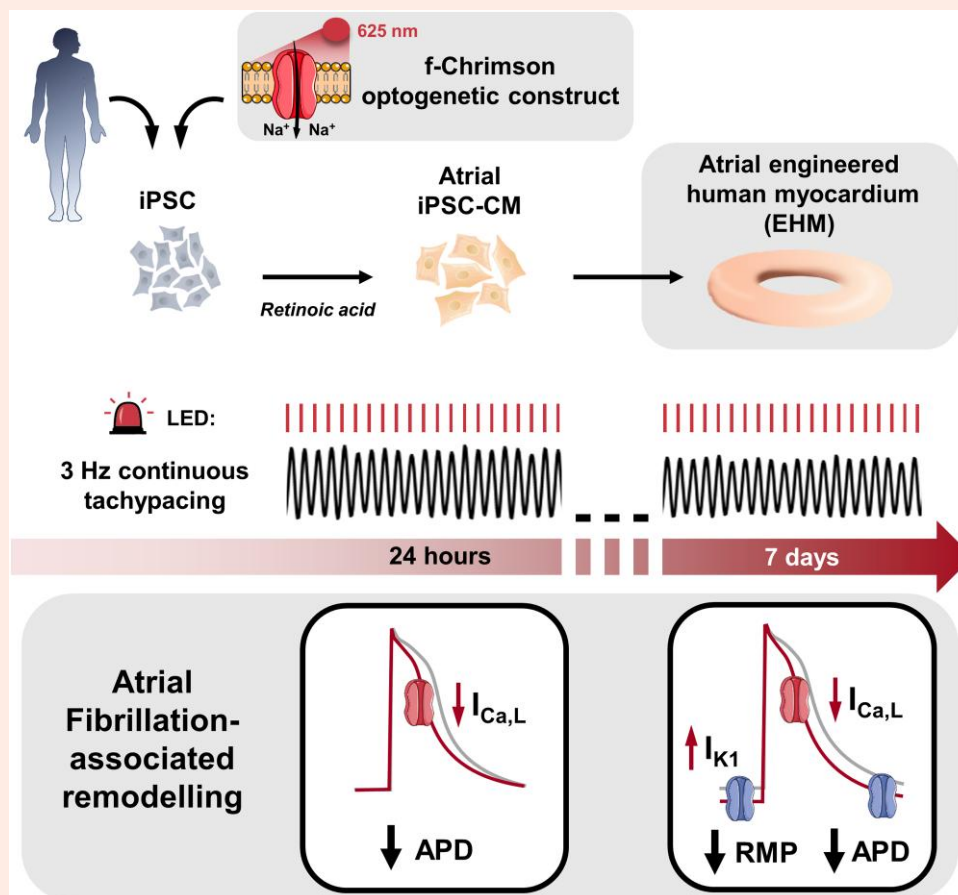
© The Author(s) 2023. Published by Oxford University Press on behalf of the European Society of Cardiology.

This is an Open Access article distributed under the terms of the Creative Commons Attribution License (<https://creativecommons.org/licenses/by/4.0/>), which permits unrestricted reuse, distribution, and reproduction in any medium, provided the original work is properly cited.

## Conclusions

Classical hallmarks of AF-associated remodelling were mimicked through TP of iPSC-aCM and aEHM. The use of the ultrafast f-Chrimson depolarizing ion channel allowed us to model the time-dependence of AF-associated remodelling *in vitro* for the first time. The observation of electrical remodelling with associated reversible contractile dysfunction offers a novel platform for human-centric discovery of antiarrhythmic therapies.

## Graphical Abstract



## Keywords

Stem cells • Ion channel • Action potential • Atrial fibrillation • Optogenetics

## 1. Introduction

Atrial fibrillation (AF) is the most frequently diagnosed cardiac arrhythmia and is associated with increased morbidity and mortality.<sup>1</sup> Therapeutic interventions have major limitations, including limited efficacy and risk of life-threatening ventricular proarrhythmic side effects. Over the last decades, major insights into underlying molecular abnormalities contributing to the initiation, maintenance, and progression of AF have been gained.<sup>1</sup> AF is associated with specific electrophysiological abnormalities that promote its sustainability and that are commonly summarized as electrical remodelling.<sup>2</sup> Accordingly, action potential (AP) shortening is a major hallmark of AF-associated electrical remodelling.<sup>3–5</sup>

To date, many mechanistic studies of AF have mainly been based on experiments in animal models.<sup>6,7</sup> However, the limitations of animal models are also apparent, including differences in basic cellular electrophysiology between humans and animals as well as the complexities underlying AF in patients. These limitations obviously limit the transferability of therapeutic

interventions from animal to human.<sup>8,9</sup> Alternatively, human atrial myocardium is available for fundamental studies of disease mechanisms, but cannot be maintained well *ex vivo* to study chronic triggers of AF or therapies. The development of atrial cardiomyocytes derived from human induced pluripotent stem cells (iPSC-aCM) promises to provide an unlimited source for *in vitro* studies of the molecular mechanisms of AF and therapeutic interventions.<sup>10–12</sup> Similar to differences observed in native cardiomyocytes, iPSC-aCM show a distinct electrophysiological phenotype when compared to ventricular iPSC-CM (iPSC-vCM).<sup>11,13,14</sup> Major differences include shorter AP duration (APD) and response to the vagal neurotransmitter acetylcholine, which is absent in ventricular cardiomyocytes.<sup>11,14</sup> However, whether AF-associated electrical remodelling can be induced in iPSC-aCM is currently unknown.

iPSC-aCM in general and atrial-engineered human myocardium (aEHM) in particular represent novel promising tools for the development of new antiarrhythmic drugs and drug testing.<sup>15–17</sup> Yet, without modelling the high frequencies of tachyarrhythmia and associated changes in ion channel

function,<sup>18,19</sup> their use in the development of novel antiarrhythmic therapies is limited. Importantly, AF-associated electrical remodelling has been shown to occur in a time-dependent manner, suggesting that chronic tachypacing (TP) would have to be introduced to simulate AF *in vitro*. For example, AF-associated increase in  $I_{K1}$  has been demonstrated to occur after 1 week or more in atrial TP<sup>20</sup> whereas remodelling of L-type  $Ca^{2+}$  current ( $I_{Ca,L}$ ) appears to be an earlier event observed over days rather than weeks.<sup>21</sup> iPSC-CM can be maintained and optically paced for longer cultivation periods<sup>22</sup> and therefore may represent an ideal model to investigate long-term responses to atrial TP *in vitro*. We, therefore, tested the hypothesis that electrical remodelling can be induced in iPSC-aCM and aEHM by using electrical and optical TP. EHM resemble a macroscale tissue format with advanced organotypic maturation and contractile function.<sup>11,23</sup>

Here we show for the first time that major characteristics of AF-associated electrical remodelling including AP shortening, reduction of  $I_{Ca,L}$  and reduced vagal neurotransmitter response can be induced in iPSC-aCM subjected to 24 h TP.<sup>24,25</sup> Furthermore, modelling chronic, uninterrupted TP (for 7 days), by making use of the newly developed ultrafast channelrhodopsin variant f-Chrimson,<sup>26</sup> was also associated with additional upregulation of the basal inward-rectifier potassium current  $I_{K1}$  and consecutive hyperpolarization of the resting membrane potential (RMP), suggesting that AF-associated electrical remodelling is time-dependent and may therefore contribute to the progression of the arrhythmia and arrhythmia-associated contractile dysfunction. Taken together, our data suggest that increased atrial stimulation frequency is a major contributor to electrical remodelling observed in patients with AF and that underlying mechanisms can be modelled in iPSC-aCM and aEHM. Our novel human 2D and 3D models coupled with TP may therefore represent powerful *in vitro* tools to simulate AF, allowing for investigation of the mechanisms underlying AF pathophysiology and potentially phenotypic screens for novel antiarrhythmic therapies.

## 2. Methods

More detailed methods are provided in the [Supplementary material online](#).

### 2.1 Human iPSC and differentiation into cardiomyocytes

iPSC-aCM and iPSC-vCM were generated by subtype-directed differentiation of iPSC from healthy donors as previously described (Figure 1).<sup>27</sup> Temporal modulation of Wnt-signalling via small molecules (G1Wi-protocol) stimulated cardiac differentiation. Atrial subtype specification was stimulated with 1  $\mu\text{mol/L}$  retinoic acid between day 3 (d3) and day 6 of differentiation. CRISPR/Cas9 (clustered regularly interspaced short palindromic repeats/Cas9 nuclease)-mediated homologous recombination was used to insert the light-gated ion-channel f-Chrimson<sup>26</sup> under the control of the CAG-promoter into the AAVS1 locus in a deeply characterized human iPSC line (TC-1133).<sup>28,29</sup> This study was performed in line with the principles of the Declaration of Helsinki. All protocols were approved by the Ethics Committee of the University Medical Center Göttingen (No. 10/9/15 and 15/2/20). Informed consent was obtained from all participants and all research was performed in accordance with relevant guidelines and regulations.

### 2.2 Generation of engineered human myocardium (EHM)

EHM was prepared as described previously (Figure 2).<sup>23,30</sup> In brief: A mixture of iPSC-CM (70%), human fibroblasts (30%) and collagen was cast into a custom made 48-well plate (myrPlate, myriamed GmbH, Germany). EHM was constructed using iPSC-CM expressing f-Chrimson (see [Supplementary material online, Figure S1](#)) unless otherwise indicated. Spontaneous contractions were observed 3–5 days after the casting procedure. EHM was maintained in a serum-free medium (SFMM) containing IMDM with Glutamax, MEM Non-Essential Amino Acids Solution, 4% B27 without insulin (all Thermo Fisher Scientific), 200  $\mu\text{mol/L}$  ascorbic acid 2-phosphate

(Sigma-Aldrich), 100 ng/mL recombinant human IGF-1, 5 ng/mL recombinant human VEGF, 10 ng/mL animal-free recombinant human FGF-basic (all PeproTech). To allow for continuous real-time monitoring of force of contraction, EHM was prepared in an alternative engineering format embedded within custom-made culture vessels each directly coupled to an isometric force sensing device as previously described.<sup>31</sup> All experiments were performed after a tissue culture period between 28 and 38 days.

### 2.3 Electrical and optical pacing of iPSC-CM and EHM

iPSC-aCM at d28 were plated onto Matrigel<sup>®</sup>-coated (1:120) 10 mm coverslips and maintained with a culture medium of RPMI 1640 with Glutamax, and 2% B27 (both Thermo Fisher Scientific) and maintained at 37°C, 5% CO<sub>2</sub>. Immediately before pacing, coverslips in a 6-well culture dish were submerged in a pacing medium of Medium 199 Glutamax (baseline  $Ca^{2+}$  concentration: 1.79 mmol/L) and 2% B27 (both Thermo Fisher Scientific). EHM mounted on stretchers were submerged in SFMM in a six-well culture dish. Electrical pacing was delivered to iPSC-aCM or aEHM at 1 or 3 Hz (always studied in parallel) for 24 h with biphasic 5 ms pulses via a C-pace EM culture stimulator (IonOptix, MA, USA).

Optical pacing was delivered via a custom-made optical pacing light emitting diode device placed above the transparent six-well culture plate lid. We quantified rheobase and chronaxie values (see [Supplementary material online, Figure S1](#)) to determine stimulation values for optical TP, which were set to 25% above contraction threshold (118  $\mu\text{W}/\text{mm}^2$  intensity, 5 ms).

Regular visual inspection at the start, after 8 h and at the end (24-h pacing) or every 24 h (7 day pacing) was undertaken to ensure cells and tissues were responsive to their supplied frequency at all investigated time-points. iPSC-aCM or aEHM were only included in this study if they passed this criterion. Seven-day contractile analysis during TP (see below) allowed for continuous real-time feedback of beating frequencies in response to pacing.

### 2.4 Optical AP recordings

Coverslips containing iPSC-CM were transferred to a  $37 \pm 0.5^\circ\text{C}$  heated chamber with bath solution containing (in mmol/L):  $CaCl_2$  2, Glucose 10, HEPES 10, KCl 4,  $MgCl_2$  1, NaCl 140; pH = 7.35 adjusted with NaOH. Cells were loaded with  $0.1 \times$  FluoVolt (Thermo Scientific; 20 min loading). Intact cells were electrically field-stimulated at 1 Hz with 3–5 ms bipolar pulses at voltages ~25% above the contraction threshold (normally between 10 and 30 V). AP were recorded optically at  $\lambda_{ex} = 470$  nm and  $\lambda_{em} = 535$  nm. Three AP from each iPSC-CM were ensemble averaged during offline analysis of AP parameters with Clampfit 10.7 (Molecular Devices, CA, USA).<sup>32</sup>

### 2.5 Patch-clamp measurements

Measurements of membrane currents were performed using conventional whole-cell ruptured-patch technique. Inward-rectifier  $K^+$  currents were recorded using the manual patch-clamp approach (Axopatch 200B, Molecular Devices) in iPSC-CM perfused with bath solution containing (in mmol/L): NaCl 120, KCl 20,  $MgCl_2$  1,  $CaCl_2$  2, glucose 10, HEPES 10; pH = 7.4 at 22–24°C. Borosilicate glass microelectrodes had tip resistances of 3–5 M $\Omega$  when filled with pipette solution (in mmol/L): K-aspartate 100, NaCl 10, KCl 40, Mg-ATP 5, EGTA 2, GTP-Tris 0.1, HEPES 10; pH = 7.4). Basal inward-rectifier  $K^+$  current was measured by applying a ramp pulse from  $-100$  to  $+40$  mV (0.5 Hz) and identified as  $Ba^{2+}$  (1 mmol/L)-sensitive current.<sup>24,25,33,34</sup>

$I_{Ca,L}$  and  $I_{Na}$  recordings were performed using an automated patch-clamp system (SyncroPatch 384, Nanion Technologies GmbH, Germany) with thin borosilicate glass, single-aperture 384-well planar fixed-well chips.<sup>13</sup>  $I_{Ca,L}$  was activated at 0.5 Hz using a voltage-step protocol with a holding potential of  $-80$  mV and a 100 ms ramp pulse to  $-40$  mV followed by a 100 ms test-pulse to  $+10$  mV at 22–24°C. The internal solution

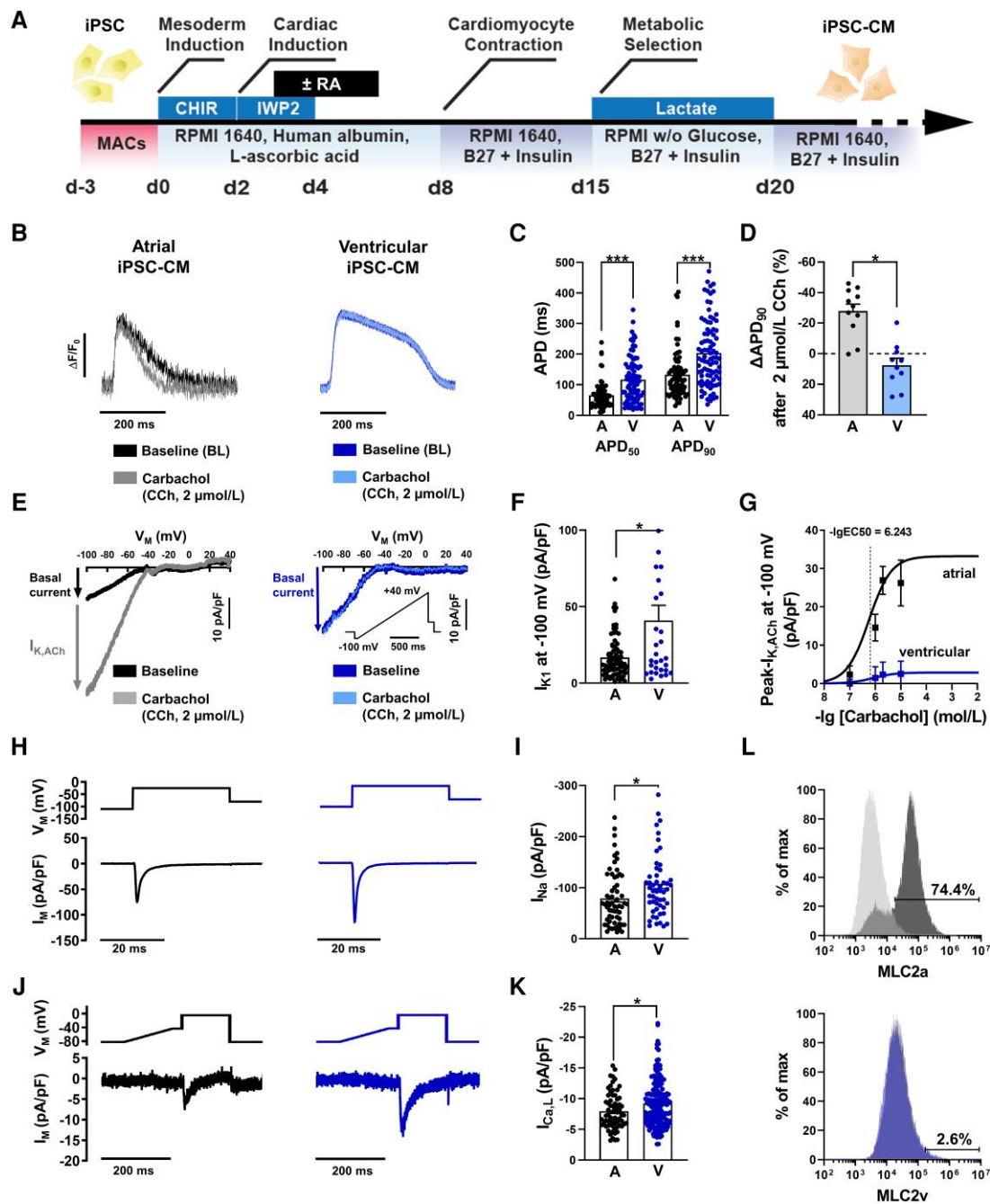


**Figure 1** Cellular electrophysiology of atrial (iPSC-aCM) and ventricular (iPSC-vCM) induced pluripotent stem cell-derived cardiomyocytes. (A) Schematic of the iPSC-CM differentiation protocols used in this study. Application of 1 μmol/L retinoic acid (RA) from day 3 (d3) to day 6 induces an atrial specific subtype. (B) Representative optical action potentials (AP) elicited at 1 Hz in intact single iPSC-aCM (A, left) and iPSC-vCM (V, right) before (baseline) and after application of the M-receptor agonist carbachol (CCh, 2 μmol/L). (C) AP duration at 50 and 90% repolarization (APD<sub>50</sub>, APD<sub>90</sub>; atrial: n = 74/4, ventricular: n = 89/3). (D) Percentage change of APD<sub>90</sub> following CCh application (atrial: n = 11/2, ventricular: n = 10/2). (E) Representative voltage-clamp recordings of inward-rectifier K<sup>+</sup> current in single iPSC-aCM (left) and iPSC-vCM (right) before (baseline, I<sub>K1</sub>) and after CCh application, revealing the acetylcholine-activated inward-rectifier K<sup>+</sup> current (I<sub>KACH</sub>) in iPSC-aCM. (F) I<sub>K1</sub> measured at -100 mV (atrial: n = 77/6, ventricular: n = 31/4). (G) Concentration-response curves for CCh-mediated activation of I<sub>KACH</sub> defined as CCh-dependent increase of inward-rectifier-K<sup>+</sup>-current amplitude at -100 mV in iPSC-aCM (n = 7-77/6) and iPSC-vCM (n = 143/1). (H), Voltage-clamp protocol (0.5 Hz, top) and representative membrane current (I<sub>M</sub>) trace (bottom) of peak Na<sup>+</sup> current (I<sub>Na</sub>) in iPSC-aCM (left) and iPSC-vCM (right). (I) Peak I<sub>Na</sub> (atrial: n = 62/1, ventricular: n = 53/1). (J) Voltage-clamp protocol (0.5 Hz, top) and representative membrane current (I<sub>M</sub>) trace (bottom) of L-type Ca<sup>2+</sup> current (I<sub>CaL</sub>) in iPSC-aCM (left) or iPSC-vCM (right). (K) Peak I<sub>CaL</sub> (atrial: n = 66/2, ventricular: n = 176/2). (L) Representative flow cytometry analysis of iPSC-aCM staining for the atrial isoform (MLC2a, top) or the ventricular isoform (MLC2v bottom) of myosin light chain. Grey peaks represent the isotype control. Data are mean ± SEM. \*P < 0.05, \*\*\*P < 0.001 vs. iPSC-aCM using unpaired Student's t-test. n/N = number of iPSC-CM/differentiation.

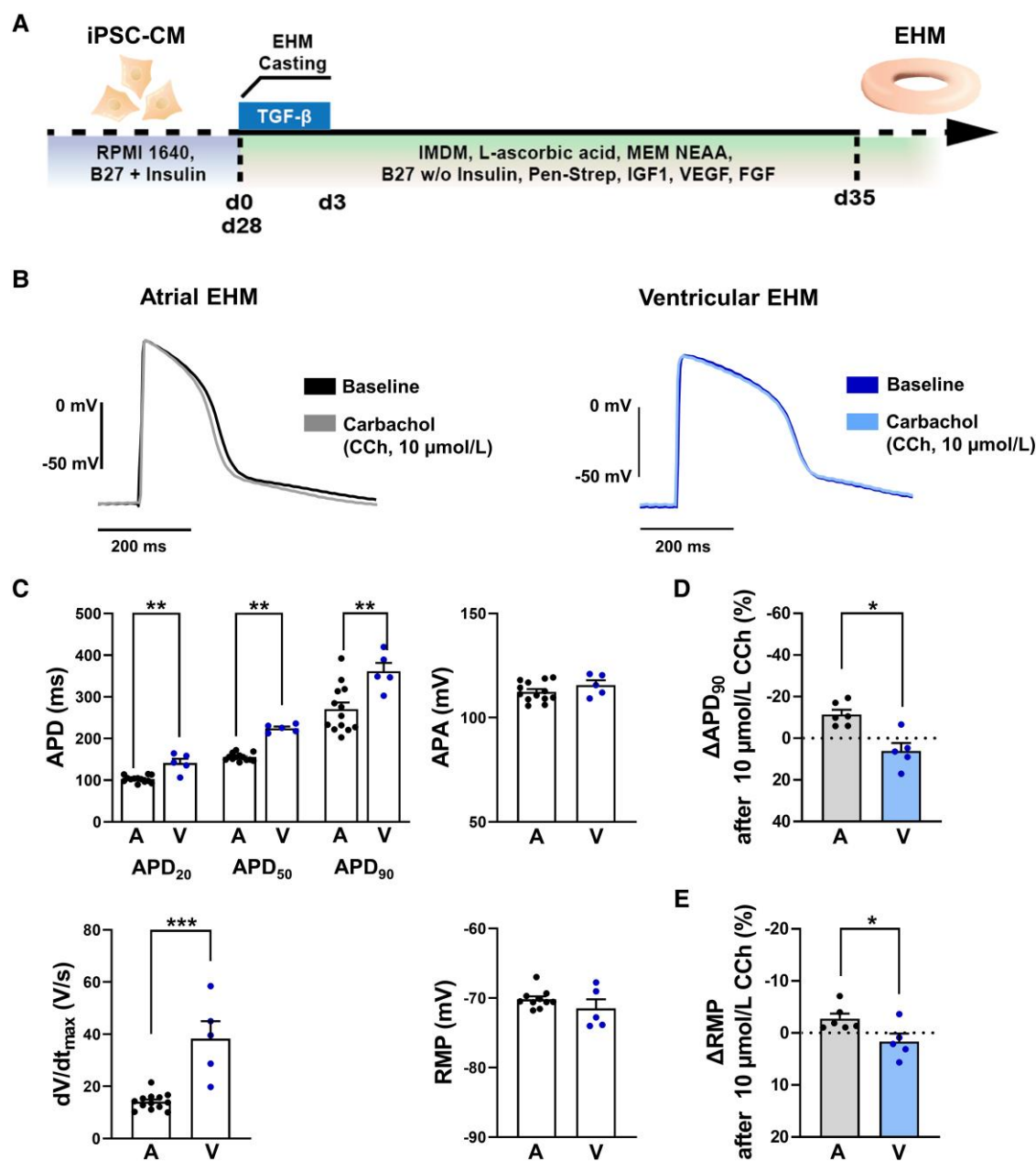


**Figure 2** Electrophysiology of atrial (aEHM) and ventricular (vEHM) engineered human myocardium. (A) Schematic of the EHM culture procedure used in this study. (B) Representative action potentials (AP) elicited at 1 Hz in aEHM (A, left) and vEHM (V, right) before (baseline) and after application of the M-receptor agonist carbachol (CCh, 10 µmol/L). (C) AP duration at 20, 50, and 90% repolarization (APD<sub>20</sub>, APD<sub>50</sub> and APD<sub>90</sub>, top left), AP amplitude (APA, top right), upstroke velocity (dV/dt<sub>max</sub>, bottom left), and resting membrane potential (RMP, bottom right; atrial: n = 13/3, ventricular: n = 5/2). (D), Percentage change of APD<sub>90</sub> following CCh application. (E), Percentage change of RMP following CCh application (atrial: n = 6/2, ventricular: n = 5/2). Data are mean ± SEM. \*P < 0.05, \*\*P < 0.01, \*\*\*P < 0.001 vs. aEHM using unpaired Student's t-test or Welch's t-test (E). n/N = number of recordings/EHM.

contained (in mmol/L): EGTA 10, HEPES 10, CsCl 10, NaCl 10, CsF 110, pH 7.2 (with CsOH). The bath solution contained (in mmol/L): HEPES 10, NaCl 140, glucose 5, KCl 4, CaCl<sub>2</sub> 2, MgCl<sub>2</sub> 1; pH = 7.4 (with KOH) at 22–24°C. I<sub>Na</sub> recordings were performed at 0.5 Hz using a voltage-step protocol with a holding potential of –100 and a 30 ms test pulse to –20 mV. Pipette solution contained (in mmol/L): EGTA 10, HEPES 10, KCl 10, NaCl 10, KF 110; pH = 7.2 (with KOH). Bath solution contained (in mmol/L HEPES 10, NaCl 140, glucose 5, KCl 4, CaCl<sub>2</sub> 2, MgCl<sub>2</sub> 1; pH = 7.4 (with KOH) at 22–24°C.

## 2.6 Sharp-electrode AP recordings

AP were recorded at 1 Hz in EHM using a Sec-05-X amplifier (npi Electronic GmbH, Germany) in voltage follower mode as previously described.<sup>35</sup> Glass-microelectrodes filled with 3 mmol/L KCl had tip resistances of 30–40 MΩ.

## 2.7 Molecular analysis

The messenger RNA (mRNA) levels of key ion channel proteins were measured by real-time PCR using standard protocols.<sup>23,36</sup> Flow cytometry

analysis of iPSC-aCM was undertaken with antibodies against the atrial (MLC2a) and the ventricular (MLC2v) isoform of myosin light chain using the BD Accuri™ C6 plus system flow cytometer (BD Biosciences, CA, USA).

## 2.8 Statistical analysis

Summarized data are reported as mean  $\pm$  standard error of the mean (SEM) unless otherwise specified. Continuous data with a sample size  $n \geq 20$  were assumed to be normally distributed (central limit theorem). Data with the sample size between  $n = 10$ – $20$  were tested for normality using the Shapiro-Wilk test. Normally distributed data were compared using unpaired two-tailed Student's *t*-test. Non-normally distributed data and all data sets with  $n < 10$ , were compared using the Mann-Whitney *U* test. Differences between data sets of unpaired data with unequal variances (F-test) were evaluated using Welch's *t*-test.

## 3. Results

### 3.1 Cardiomyocytes and EHM with distinct atrial properties derived from human iPSC

Spontaneous beating frequency was higher in atrial compared to ventricular iPSC-CM (see [Supplementary material online, Figure S2](#)) as previously reported.<sup>11</sup> In order to prevent frequency-dependent bias on AP parameters and ion channel properties, electrophysiological experiments were performed at defined stimulation frequencies throughout the study. We first assessed optical AP characteristics of intact, single atrial and ventricular iPSC-CM under 1 Hz field stimulation. As anticipated, APD at 50 and 90% repolarization (APD<sub>50</sub>, APD<sub>90</sub>) was shorter in iPSC-aCM compared to iPSC-vCM ([Figure 1B and C](#)). In native myocardium, vagal nerve stimulation shortens the atrial, but not ventricular AP.<sup>37</sup> Accordingly, application of the muscarinic-receptor (M-receptor) agonist carbachol (CCh, 2  $\mu$ mol/L) resulted in AP shortening in atrial, but not in ventricular iPSC-CM ([Figure 1B and D](#)).

AP shortening in response to M-receptor stimulation is mediated through activation of acetylcholine-activated inwardly rectifying K<sup>+</sup> channels (I<sub>K,ACh</sub>).<sup>24,25,38,39</sup> In agreement with this observation, mRNA levels of the corresponding channel subunit Kir3.1 (KCNJ3) were two-times higher in atrial vs. ventricular iPSC-CM (see [Supplementary material online, Figure S3](#)). In order to directly measure I<sub>K,ACh</sub> in iPSC-CM, we employed a previously described patch-clamp depolarizing ramp protocol.<sup>25,40</sup> Representative recordings in the absence of M-receptor agonists showed typical inward-rectifier properties in response to the depolarizing ramp-protocol with high conductance in the inward branch, which represents basal inward-rectifier K<sup>+</sup> current I<sub>K1</sub> ([Figure 1E](#)). As expected from reports on native human atrial and ventricular cardiomyocytes, I<sub>K1</sub> was about 40% smaller in atrial vs. ventricular iPSC-CM ([Figure 1F](#)).<sup>41,42</sup> However, only in iPSC-aCM did the application of CCh result in an increase in total current density (labelled I<sub>K,ACh</sub>) in a concentration-dependent manner (-lgEC<sub>50</sub> = 6.24  $\pm$  0.7 mol/L [571 nmol/L]; [Figure 1E and G](#), [Supplementary material online, Figure S4](#)). In addition, despite the continuous presence of the M-receptor agonist, in iPSC-aCM I<sub>K,ACh</sub> decreased from a 'peak'-value to a 'quasi-steady state' (QSS) level within two minutes in a biphasic manner (see [Supplementary material online, Figure S4](#)). The QSS/Peak ratio (0.55  $\pm$  0.03,  $n = 77$ ) was similar to our earlier reports using native human atrial cardiomyocytes indicating comparable underlying mechanisms.<sup>24,25</sup> Apart from canonical M-receptor mediated activation of I<sub>K,ACh</sub>, adenosine receptors can also activate cardiac I<sub>K,ACh</sub> channels. Accordingly, adenosine activated K<sup>+</sup> channels in iPSC-aCM in a concentration-dependent manner (-lgEC<sub>50</sub> = 6.04  $\pm$  0.4 mol/L [898 nmol/L]), whereas no effect was observed in iPSC-vCM (see [Supplementary material online, Figure S4](#)). Amplitudes of both I<sub>Na</sub> ([Figure 1H and I](#)) and I<sub>Ca,L</sub> ([Figure 1J and K](#)) were smaller in iPSC-aCM, with the latter potentially contributing to the shorter atrial APD (see [Supplementary material online, Figure S5](#)). Functional characterization of iPSC-aCM was supplemented with molecular analysis indicating minimal (2.6%) contamination of iPSC-vCM in the atrial cellular

cohort. This was also confirmed by high throughput functional screening of I<sub>K,ACh</sub> (see [Supplementary material online, Figure S6](#)).

In order to generate a multicellular, matured heart muscle environment, we next generated EHM from iPSC-aCM (aEHM) and iPSC-vCM (vEHM) ([Figure 2A](#)). Compared to vEHM, aEHM had a shorter APD ([Figure 2B and C](#)) and a smaller AP upstroke velocity. Application of 10  $\mu$ mol/L CCh elicited significant shortening of APD<sub>90</sub> and hyperpolarization of the RMP only in aEHM, not in vEHM. Taken together, this indicates the atrial phenotype is conserved in aEHM. Spontaneous beating has previously been shown to be faster in aEHM compared to vEHM,<sup>11</sup> and is shown in [Supplementary material online, Video S1 and Video S2](#), respectively.

### 3.2 AP shortening and reduced I<sub>Ca,L</sub> in iPSC-aCM and aEHM subjected to 24 h TP

In AF patients, sustained atrial tachycardia leads to electrical and structural remodelling that promotes chronification of AF.<sup>1</sup> We therefore tested whether iPSC-aCM are also prone to develop electrical remodelling in response to *in vitro* TP. In agreement with our hypothesis, 24-h TP with 3 Hz to simulate atrial tachycardia<sup>38</sup> resulted in shortening of the APD<sub>50</sub> and APD<sub>90</sub> in iPSC-aCM in comparison to controls subjected to 1 Hz pacing ([Figure 3A and B](#)). I<sub>Ca,L</sub> amplitude was significantly reduced after 24-h TP ([Figure 3C and D](#)), suggesting that reduced depolarizing I<sub>Ca,L</sub> could play a role in TP-dependent APD shortening (see [Supplementary material online, Figure S5](#)). TP-induced remodelling of I<sub>Ca,L</sub> was independent of recording temperature (see [Supplementary material online, Figure S7](#)). Total Ca<sup>2+</sup> influx was estimated by quantifying the area under the curve of the I<sub>Ca,L</sub>.<sup>43</sup> Ca<sup>2+</sup>-influx was reduced by 23% in iPSC-aCM subjected to TP, which is considered a protective mechanism to limit detrimental Ca<sup>2+</sup> overload during TP.<sup>24,38</sup> We therefore hypothesized that TP-induced Ca<sup>2+</sup> overload may be an important elicitor of electrical remodelling in iPSC-aCM. Accordingly, TP-induced AP shortening was absent following pacing in a low Ca<sup>2+</sup> environment pointing to a Ca<sup>2+</sup>-mediated mechanism underlying TP-induced electrical remodelling in iPSC-aCM (see [Supplementary material online, Figure S8](#)). Hypophosphorylation of L-type Ca<sup>2+</sup> channels has been consistently suggested as a potential contributor to I<sub>Ca,L</sub> downregulation by various studies in samples from AF patients.<sup>5</sup> In order to test whether reduced phosphorylation of I<sub>Ca,L</sub> channels may also contribute to I<sub>Ca,L</sub> downregulation in our model, we investigated the effects of type 1 and type 2A phosphatase inhibitor okadaic acid (OA, 1  $\mu$ mol/L) on I<sub>Ca,L</sub> in iPSC-aCM subjected to 24 h TP. Similar to observations in atrial cardiac myocytes from patients with AF, OA increased I<sub>Ca,L</sub> amplitude only in iPSC-aCM paced at 3 Hz, not in the 1 Hz paced group pointing to an altered phosphorylation-dependent regulation of I<sub>Ca,L</sub> ([Figure 3E and F](#)).

Following 24-h optical TP of aEHM, significant shortening of APD<sub>50</sub> and APD<sub>90</sub> was observed, but no TP-dependent effects were detected in RMP, AP upstroke velocity and AP amplitude (APA) ([Figure 3G and H](#)). This was also reflected in electrical pacing of aEHM (see [Supplementary material online, Figure S9](#)). The extent of electrical remodelling and AP shortening in aEHM was not altered by arrhythmogenic pacing, in which an irregular frequency is applied deviating with 50% variability from a 3 Hz mean (see [Supplementary material online, Figure S10](#)). TP-induced remodelling involving reduced I<sub>Ca,L</sub> and a shorter AP was also observed in iPSC-vCM and vEHM, respectively, (see [Supplementary material online, Figure S11](#)) aligning with a previous study.<sup>22</sup> This indicates that I<sub>Ca,L</sub> downregulation is a common mechanism to prevent Ca<sup>2+</sup> overload in response to tachycardia.

### 3.3 Response to vagal neurotransmitters is impaired in iPSC-aCM and aEHM subjected to 24 h TP

APD shortening in response to application of M-receptor agonists such as CCh is a classical hallmark of atrial cardiomyocytes ([Figure 1B and D](#)). Furthermore, it is well known that this response is blunted in atrial cardiomyocytes from patients with AF.<sup>24,25</sup> We, therefore, analysed AP response of iPSC-aCM subjected to 24-h TP to application of the M-receptor agonist CCh. Whereas CCh induced significant AP shortening in control iPSC-aCM paced at 1 Hz, this effect was abolished in the TP

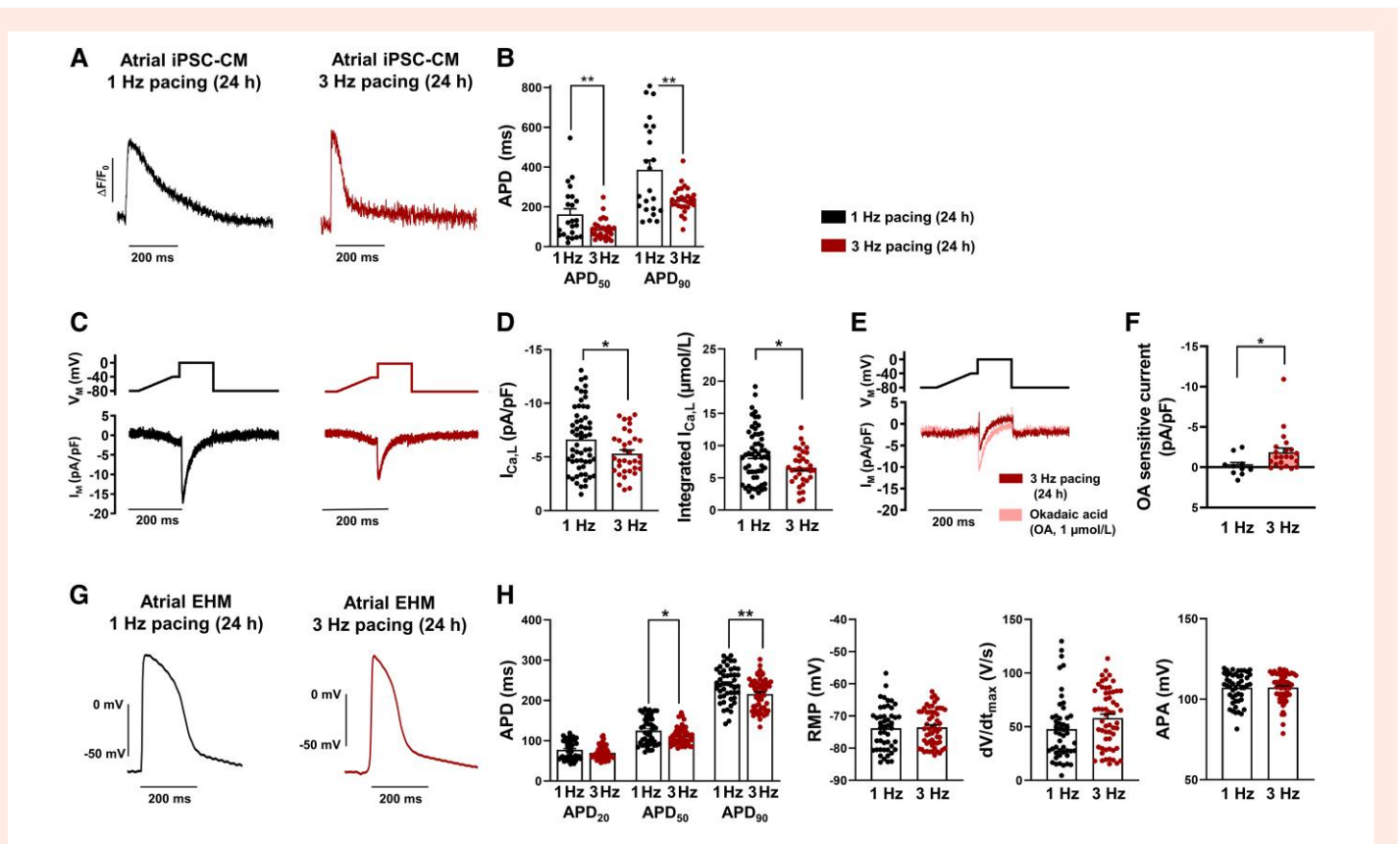


**Figure 3** Twenty-four hour TP-induced remodelling of cellular electrophysiology in atrial induced pluripotent stem cell-derived cardiomyocytes (iPSC-aCM) and atrial engineered human myocardium (aEHM). (A) Representative optical action potentials (AP) elicited at 1 Hz in intact single iPSC-aCM after 24 h electrical pacing at 1 Hz (left) or 3 Hz (right). (B) AP duration at 50 and 90% repolarization ( $APD_{50}$ ,  $APD_{90}$ , 1 Hz:  $n = 23/3$ , 3 Hz:  $n = 28/3$ ) (C), Voltage-clamp protocol (0.5 Hz, top) and representative membrane current ( $I_m$ ) trace (bottom) of L-type  $Ca^{2+}$  current ( $I_{Ca,L}$ ) in iPSC-aCM after 24 h electrical pacing at 1 Hz (left) or 3 Hz (right). (D), Peak  $I_{Ca,L}$  (left), integrated  $I_{Ca,L}$  expressed as estimated cytosolic  $Ca^{2+}$  influx (right; 1 Hz:  $n = 23/4$ , 3 Hz:  $n = 28/4$ ). (E), Voltage-clamp protocol (0.5 Hz, top) and representative membrane current ( $I_m$ ) trace (bottom) of  $I_{Ca,L}$  in 24 h 3 Hz paced iPSC-aCM before and after application of type 1 and type 2A phosphatase inhibitor okadaic acid (OA, 1  $\mu\text{mol/L}$ ). (F), Change in peak  $I_{Ca,L}$  following OA application (1 Hz:  $n = 11/1$ , 3 Hz:  $n = 22/1$ ). (G) Representative AP were elicited at 1 Hz in aEHM after 24 h optical pacing at 1 Hz (left) or 3 Hz (right). (H)  $APD_{20}$ ,  $APD_{50}$  and  $APD_{90}$  (left), resting membrane potential (RMP, middle left), upstroke velocity ( $dV/dt_{max}$ , middle right), AP amplitude (APA, right; 1 Hz:  $n = 49/14$ , 3 Hz:  $n = 61/15$ ). Data are mean  $\pm$  SEM. \* $P < 0.05$ , \*\* $P < 0.01$  vs. 1 Hz using unpaired Student's t-test or Welch's t-test (F).  $n/N$  = number of iPSC-CM/differentiation or number of recordings/EHM.

group (Figure 4A and B). To further unravel the underlying ion-channel remodelling, we quantified alterations of inward-rectifier  $K^+$  currents in response to 24-h TP. In the absence of CCh, inward-rectifier  $K^+$  current amplitude, which is mainly controlled by  $I_{K1}$  channels, was unaltered in response to 24-h TP (Figure 4C and D). In contrast, application of CCh resulted in a smaller current increase in the 24-h TP group pointing to reduced  $I_{K_{ACH}}$  current amplitude (Figure 4C, E), resembling AF-associated remodelling. Importantly, in iPSC-aCM subjected to TP,  $I_{K_{ACH}}$  recovered from TP-induced remodelling within additional 24-h normofrequent pacing at 1 Hz (see Supplementary material online, Figure S12). AP response to CCh was also restored in TP iPSC-aCM following an additional 24 h of 1 Hz pacing (see Supplementary material online, Figure S12).

It has been shown that atrial cardiomyocytes from patients with AF develop agonist-independent constitutive  $I_{K_{ACH}}$  ( $I_{K_{ACH,c}}$ ), which has been suggested to contribute to AP shortening in these patients.<sup>25,38,39</sup> Since  $I_{K_{ACH}}$  channels are not expressed in ventricular myocytes,  $I_{K_{ACH,c}}$  represents a potential atrial- and pathology-specific drug target. To unmask  $I_{K_{ACH,c}}$  in iPSC-aCM subjected to TP, we applied the selective  $I_{K_{ACH}}$  blocker tertipatin (TTP) (100 nmol/L). In the absence of M-receptor agonists, TTP reduced the basal inward-rectifier  $K^+$  current in the TP group, but was without effect in control iPSC-aCM subjected to 24-h pacing at

1 Hz (Figure 4F and G). Both the reduced agonist-dependent  $I_{K_{ACH}}$  and the development of agonist-independent constitutive  $I_{K_{ACH}}$  as observed in iPSC-aCM subjected to 24-h TP are classical hallmarks of AF-associated remodelling. These features were absent in iPSC-aCM subjected to TP in low  $Ca^{2+}$  (0.42 mmol/L) conditions, suggesting that TP-induced remodelling of  $I_{K_{ACH}}$  in iPSC-aCM is  $Ca^{2+}$  dependent (see Supplementary material online, Figure S8).

CCh (10  $\mu\text{mol/L}$ ) application to aEHM subjected to 24 h optical normofrequent pacing at 1 Hz shortened APD and hyperpolarized RMP (Figure 4H and I, Supplementary material online, Figure S13). These effects are thought to be mainly mediated by activation of  $I_{K_{ACH}}$  as observed in myocytes isolated from aEHM (see Supplementary material online, Figure S4). In contrast, the response to CCh was completely blunted after 24-hour TP of aEHM pointing to impaired  $I_{K_{ACH}}$  channel activity (Figure 4E and F).

### 3.4 Molecular features of aEHM after 24 h TP

In order to investigate the molecular basis of the observed electrophysiological phenotype and to determine whether alterations in ion-channel expression resemble those observed in patients with persistent AF, we

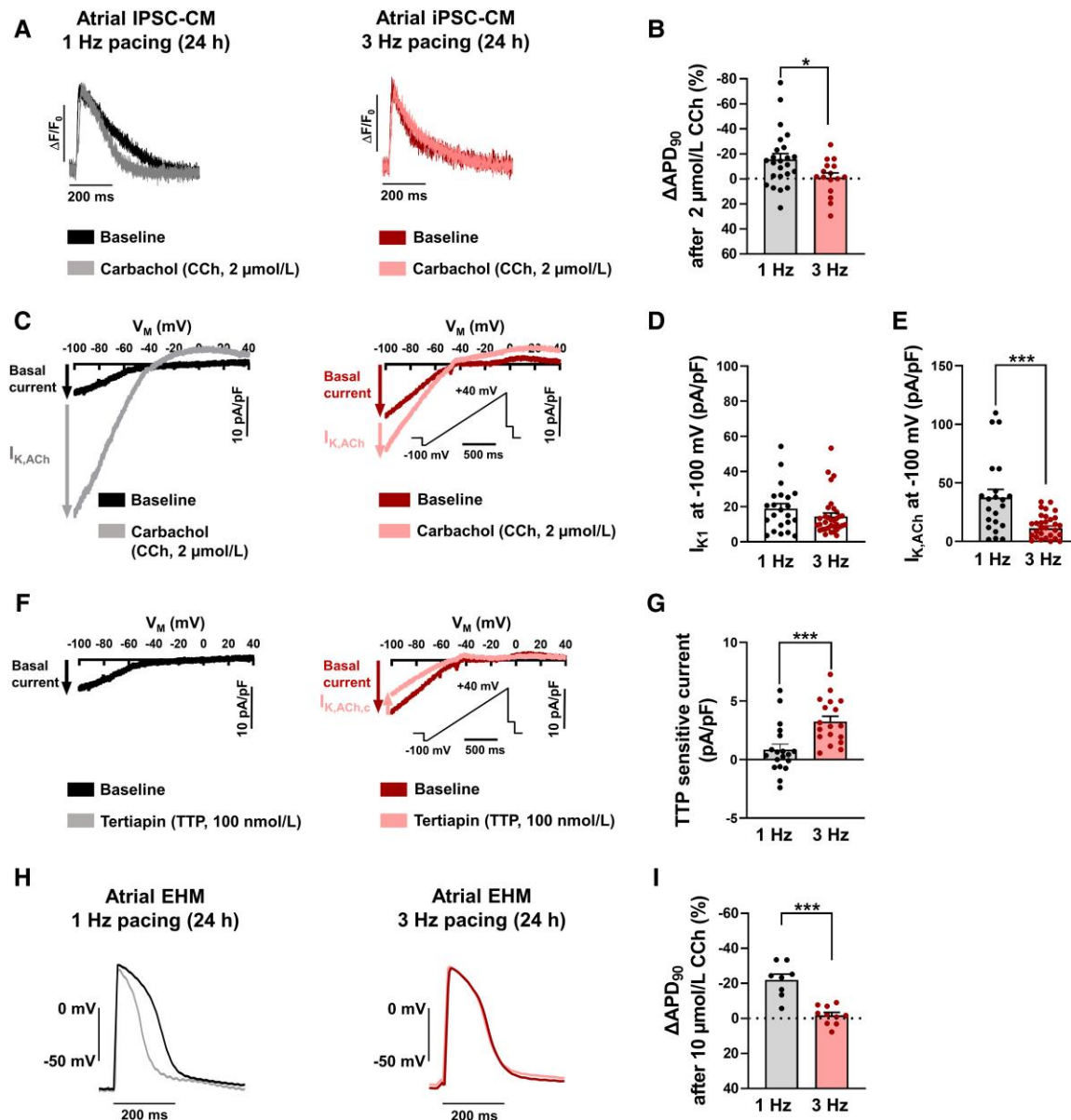


**Figure 4** Twenty-four hour TP-induced remodelling of inward-rectifier K<sup>+</sup> currents in atrial induced pluripotent stem cell-derived cardiomyocytes (iPSC-aCM) and atrial engineered human myocardium (aEHM). (A), Representative optical action potentials (AP) elicited at 1 Hz in intact single iPSC-aCM after 24 h electrical pacing at 1 Hz (left) or 3 Hz (right) before (baseline) and after application of the M-receptor agonist carbachol (CCh, 2 μmol/L). (B), Percentage change of AP duration at 90% repolarization (APD<sub>90</sub>) following CCh application (1 Hz: 26/4, 3 Hz: n = 16/3). (C), Representative voltage-clamp recordings of inward-rectifier K<sup>+</sup> current in single iPSC-aCM after 24 h electrical pacing at 1 Hz (left) or 3 Hz (right) before (baseline, I<sub>K1</sub>) and after CCh application, revealing the acetylcholine-activated inward-rectifier K<sup>+</sup> current (I<sub>K,ACh</sub>). (D), Peak I<sub>K1</sub> measured at -100 mV. E, Peak I<sub>K,ACh</sub> measured at -100 mV (D, E: 1 Hz: n = 22/2, 3 Hz: n = 34/2). (F), Representative voltage-clamp recordings of basal inward-rectifier K<sup>+</sup> current in single iPSC-aCM after 24 h electrical pacing at 1 Hz (left) or 3 Hz (right) before (baseline) and after application of selective I<sub>K,ACh</sub> blocker tertiapin (TTP, 100 nmol/L). (G), Change in basal current at -100 mV following TTP application, defined as agonist independent constitutive I<sub>K,ACh</sub> (I<sub>K,ACh,c</sub>; 1 Hz: n = 19/2, 3 Hz: n = 18/2). (H), Representative AP elicited at 1 Hz in aEHM after 24 h optical pacing at 1 Hz (left) or 3 Hz (right) before and after CCh application (10 μmol/L). (I), Percentage change of APD<sub>90</sub> following CCh application (1 Hz: n = 8/5, 3 Hz: n = 10/5). Data are mean ± SEM. \*P < 0.05, \*\*\*P < 0.001 vs. 1 Hz using paired Student's t-test. n/N = number of iPSC-CM/differentiation or number of recordings/EHM.

quantified the expression of corresponding mRNA in aEHM subjected to optical TP (Figure 5A). Similar to persistent AF patients,<sup>5</sup> expression of *CACNA1C* was unaltered suggesting that reduced I<sub>Ca,L</sub> in aEHM subjected to TP is due to additional post-translational mechanisms such as hypophosphorylation (Figure 3E and F). In accordance with unaltered I<sub>K1</sub> current in

iPSC-aCM subjected to TP (Figure 3C and D), TP was without effect on the corresponding mRNA (*KCNJ2*).

In atrial myocytes, the I<sub>K,ACh</sub> channel is a heterotetrameric complex composed of Kir3.1 and Kir3.4 subunits. TP-induced remodelling reduced the expression of *KCNJ5* mRNA encoding for Kir3.4 but had no effect on



*KCNJ3* mRNA encoding for Kir3.1. Therefore, similar to observations in patients with persistent AF,<sup>34</sup> impaired CCh response in aEHM subjected to TP appears to be mainly due to downregulation of the Kir3.4 channel subunit with less or absent reduction in Kir3.1 expression, respectively (Figure 5B). Expression of M-receptor subtype 2 (M2) and adenosine receptor (A1), which mediate activation of  $I_{K_{ACH}}$  in response to CCh and adenosine, respectively, was unaltered by TP (Figure 5C). This is in accordance with previous publications showing unaltered M2-receptor expression in patients with AF,<sup>44</sup> suggesting that in both models reduced expression of  $I_{K_{ACH}}$  channels together with development of constitutive activity are the major contributors to reduced activation of  $I_{K_{ACH}}$  in response to CCh.

### 3.5 Seven-day Continuous TP of iPSC-aCM and aEHM reveals RMP hyperpolarization and $I_{K1}$ upregulation

A major characteristic of AF is its chronically progressive nature. Whereas AF initially occurs as self-terminating episodes, i.e. paroxysmal AF, later stages of AF are characterized by the continuous persistence of the arrhythmia. Persistent AF is classified when episodes last longer than 7 days. The clinical progression of the arrhythmia is associated with progression of electrical remodelling.<sup>2</sup>

Prolonged optical TP for 7 days resulted in a marked decrease of APD<sub>50</sub> and APD<sub>90</sub> in aEHM (Figure 6A and B). In addition, 7-day TP led to hyperpolarization of the RMP and an increase in APA. Both alterations were absent after short-term 24-h TP. Hyperpolarization of the RMP represents another hallmark of AF-associated remodelling which is likely due to  $I_{K1}$  upregulation.<sup>24,35</sup> Indeed, basal inward-rectifier current was significantly higher in iPSC-aCM subjected to 3 Hz TP for 7 days compared to iPSC-aCM paced at 1 Hz for 7 days (Figure 6C and D). The hyperpolarized RMP and

increased  $I_{K1}$  observed after 7-day, but not after 24-h, TP suggest a different time-course in electrical remodelling in response to TP. Finally, AP response to CCh was blunted in aEHM after 7-day TP (see [Supplementary material online, Figure S14](#)).

### 3.6 Reduced contractility in aEHM after continuous 7-day TP

aEHM were maintained inside force sensing culture vessels which were optically stimulated for 7 days at 1 Hz or 3 Hz. Force of contraction was measured at 1 Hz every 24 h (Figure 7A). Seven-day TP significantly reduced the force of contraction in comparison to control tissues stimulated at 1 Hz (Figure 7B–G). A clear reduction in force of contraction after only 1 day of TP is consistent with the decreased  $I_{Ca,L}$  observed after only 24-h TP in iPSC-aCM (Figure 3C and D) which could potentially influence the contractile properties of the cells. Furthermore, the reduction in force of contraction after 7 days of TP was reversible after a further 7 days of 1 Hz pacing (see [Supplementary material online, Figure S15](#)), suggesting that the initial contractility reduction during TP is unlikely to be caused by irreversible structural alterations such as increased apoptosis or fibrosis.

## 4. Discussion

In this study, we tested the hypothesis that iPSC-aCM and aEHM undergo electrical remodelling under TP, resembling phenotypic changes observed in patients with AF. We found that 24-h TP is sufficient to induce AP shortening in iPSC-aCM and aEHM, which is likely due to reduced  $I_{Ca,L}$  amplitude. In addition, 24-h TP blunted the response to CCh in both iPSC-aCM and aEHM, which is compatible with reduced agonist-dependent  $I_{K_{ACH}}$  activation and development of agonist-independent constitutive  $I_{K_{ACH}}$

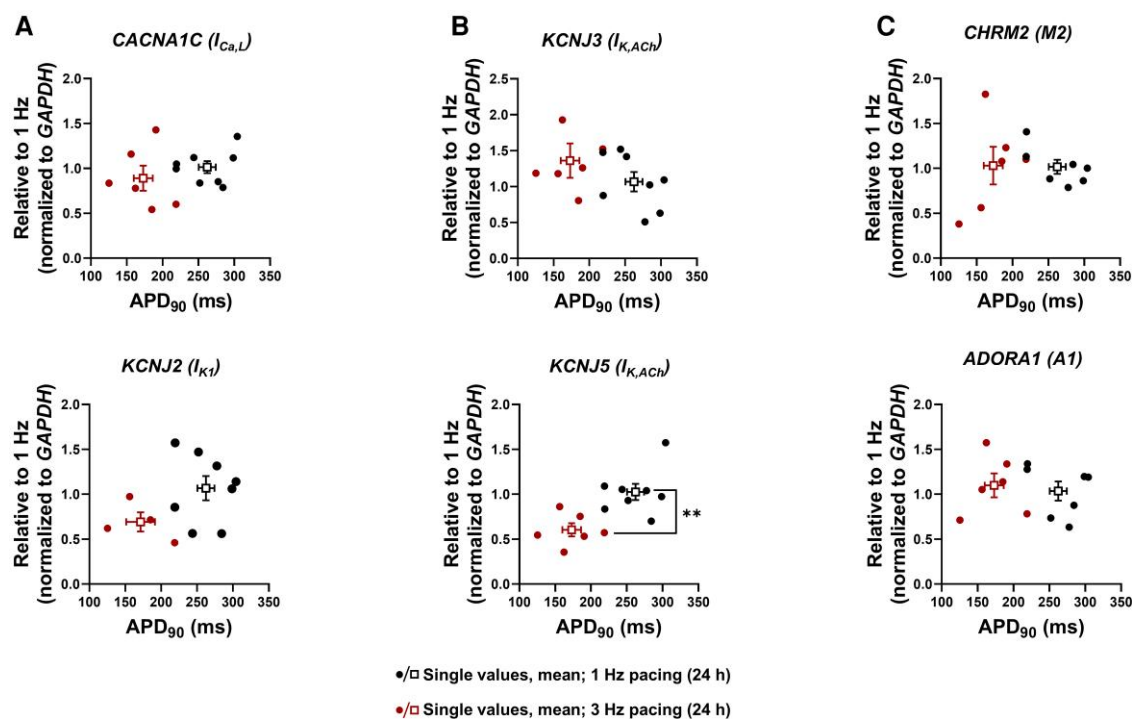


**Figure 5** Gene expression of ionic channels and receptors in atrial engineered human myocardium (aEHM) subjected to 24-h optical TP. (A), mRNA levels of ion channels *CACNA1C* ( $I_{Ca,L}$ , top) and *KCNJ2* ( $I_{K1}$ , bottom). (B), mRNA levels of  $I_{K_{ACH}}$  ion channel subunits *KCNJ3* (top) and *KCNJ5* (bottom). (C), mRNA levels of receptors *CHRM2* (M2 receptor, top) and *ADORA1* (A1 receptor, bottom). All values are plotted as single values against the corresponding action potential duration at 90% repolarization (APD<sub>90</sub>). Data are mean  $\pm$  SEM. \*\* $P < 0.01$  vs. 1 Hz using the Mann-Whitney U test.

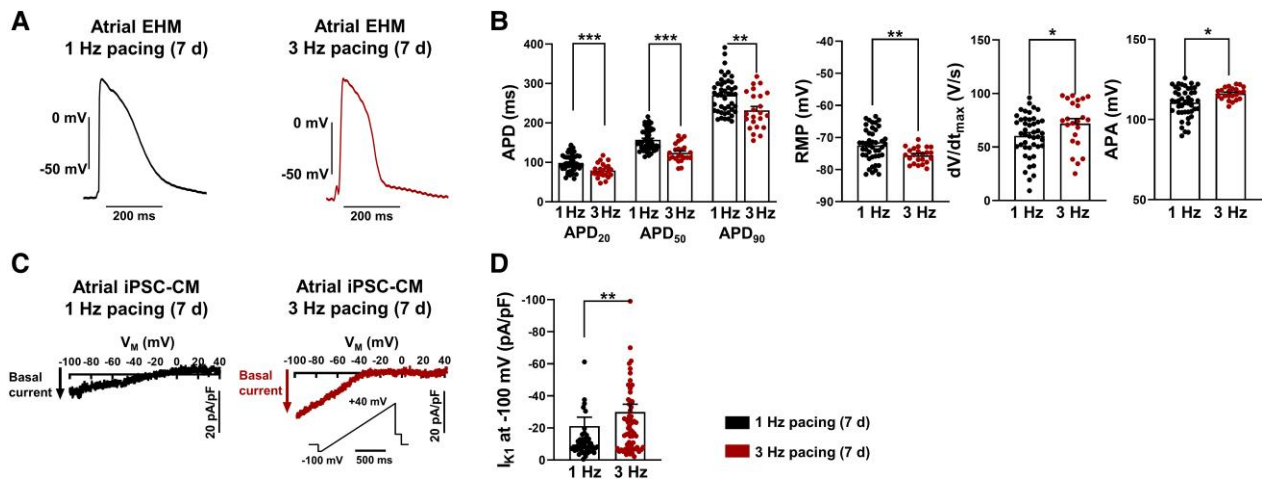


**Figure 6** Prolonged (7-day) TP-induced remodelling of cellular electrophysiology in atrial engineered human myocardium (aEHM) and atrial induced pluripotent stem cell-derived cardiomyocytes (iPSC-aCM). (A), Representative action potentials (AP) elicited at 1 Hz in aEHM after 7 days of optical pacing at 1 Hz (left) or 3 Hz (right). (B), AP duration at 20, 50, and 90% repolarization (APD<sub>20</sub>, APD<sub>50</sub> and APD<sub>90</sub>, left), resting membrane potential (RMP, middle left), upstroke velocity (dV/dt<sub>max</sub>, middle right), AP amplitude (APA, right; 1 Hz: n = 45/8, 3 Hz: n = 23/9). (C) Representative voltage-clamp recordings of basal inward-rectifier K<sup>+</sup> current (I<sub>K1</sub>) current in iPSC-aCM after 7 day of optical pacing at 1 Hz (left) or 3 Hz (right). (D) Peak I<sub>K1</sub> measured at -100 mV (1 Hz: n = 49/1, 3 Hz: n = 64/1). Data are mean ± SEM. \*P < 0.05, \*\*P < 0.01, \*\*\*P < 0.001 vs. 1 Hz using paired Student's t-test. n/N = number of iPSC-CM/differentiation or number of recordings/EHM.

activity (I<sub>K<sub>ACh,c</sub>) in patients with AF. In contrast, 24-h TP was not sufficient to induce RMP hyperpolarization, which was observed after 7-day TP only, pointing to time-dependent development of specific hallmarks of electrical remodelling. Our data clearly demonstrate that several major hallmarks of AF-associated remodelling can be reproduced in iPSC-aCM and aEHM by electrical and optical TP.</sub>

#### 4.1 AF-associated electrical remodelling

It is well known that AF is a progressive disease.<sup>1,2</sup> Initially, AF often occurs as paroxysmal AF when episodes last less than 7 days and terminate spontaneously. However, with increasing duration of the rhythm disturbance, AF proceeds to become 'persistent' when conversion to sinus rhythm can only be achieved with pharmacological or electrical interventions, and 'permanent' when no further attempts to restore sinus rhythm are considered clinically useful.<sup>45</sup> The progression of AF to more severe stages makes treatment of the arrhythmia in particular difficult. For many years there has been hope that unravelling the mechanisms underlying AF progression may lead to safer and more effective therapeutic rhythm control strategies.<sup>1,46</sup>

Wijffels *et al.* first demonstrated in a goat model that experimentally maintained AF alters atrial electrophysiology in a way that promotes persistence of the arrhythmia, thereby demonstrating that 'AF begets AF'.<sup>47</sup> In particular, the authors demonstrated that atrial TP led to shortening of the effective refractory period and coined the term 'electrical remodelling' to describe AF-promoting changes caused by AF itself.

In patients, decreased I<sub>Ca,L</sub> and increased inward-rectifier K<sup>+</sup> current I<sub>K1</sub> are major hallmarks of electrical remodelling that lead to APD shortening and hyperpolarization of the RMP, respectively.<sup>3-5,35,48,49</sup> In addition, reduced amplitude of the acetylcholine-activated inward-rectifier K<sup>+</sup> current I<sub>K<sub>ACh</sub> and development of its agonist independent constitutive activity represent well-accepted components of electrical remodelling in patients with AF.<sup>24,25,33,38</sup></sub>

It is believed that the very rapid atrial activity in AF represents a major driver for electrical remodelling.<sup>21,24,38</sup> In fact, remodelling induced by AF is virtually indistinguishable from that produced by electrical

tachycardia, and electrical TP of animal models has become one of the most accepted approaches to study mechanisms underlying AF-associated remodelling.<sup>6,7</sup> TP-induced remodelling has since been demonstrated in dogs,<sup>38,39,50</sup> sheep,<sup>51,52</sup> rabbits,<sup>53</sup> goats<sup>47</sup> and pigs,<sup>54</sup> where application of TP between 1 and 2 weeks leads to shortening of both effective refractory period and APD causing increased vulnerability to AF induction and increased arrhythmia persistence. Similar to AF patients, atrial myocytes isolated from those models show reduced I<sub>Ca,L</sub>, increased I<sub>K1</sub> and reduced agonist-dependent I<sub>K<sub>ACh</sub> as classical hallmarks of electrical remodelling.</sub>

In addition to the reduced activation of I<sub>K<sub>ACh</sub> by M-receptor agonists, increased opening of agonist-independent constitutively active I<sub>K<sub>ACh</sub> channels is a major characteristic of electrical remodelling in AF patients and animal models of AF.<sup>24,25,33,38,39</sup> I<sub>K<sub>ACh,c</sub> contributes to the basal inward-rectifier K<sup>+</sup> current in AF and can be unmasked using the selective I<sub>K<sub>ACh</sub> inhibitor TTP as shown in atrial myocytes from AF patients and animal models as well as in the present study (Figure 4).<sup>55</sup> TTP also terminates AF without affecting ventricular electrophysiology, indicating that I<sub>K<sub>ACh,c</sub> may be a potentially interesting anti-arrhythmic target.<sup>56</sup> Consistent with previous data,<sup>24,38</sup> our experiments suggest that development of I<sub>K<sub>ACh,c</sub> involves Ca<sup>2+</sup>-dependent mechanisms since I<sub>K<sub>ACh,c</sub> was absent in response to TP in a low Ca<sup>2+</sup> pacing environment (see [Supplementary material online, Figure S8](#)). As shown in dog atrial myocytes and patients with AF, the rate-induced Ca<sup>2+</sup> overload is thought to activate calpain that cleaves cell proteins and leads to the breakdown of the I<sub>K<sub>ACh</sub> inhibitory protein kinase C alpha.<sup>24,38</sup> Together with increased membrane translocation of the stimulatory protein kinase C epsilon, these mechanisms are likely to contribute to I<sub>K<sub>ACh</sub> remodelling in AF and TP models.<sup>38,57</sup></sub></sub></sub></sub></sub></sub></sub></sub></sub>

#### 4.2 iPSC-aCM and aEHM as AF models

Over the past few years, we have learnt a great deal about molecular mechanisms underlying the initiation and maintenance of AF, by studying right atrial biopsies from patients undergoing open heart surgery.<sup>1,2,58</sup> Studying human atrial samples mainly allows for the bare description of the arrhythmogenic substrate, whereas interventions that modify development of an

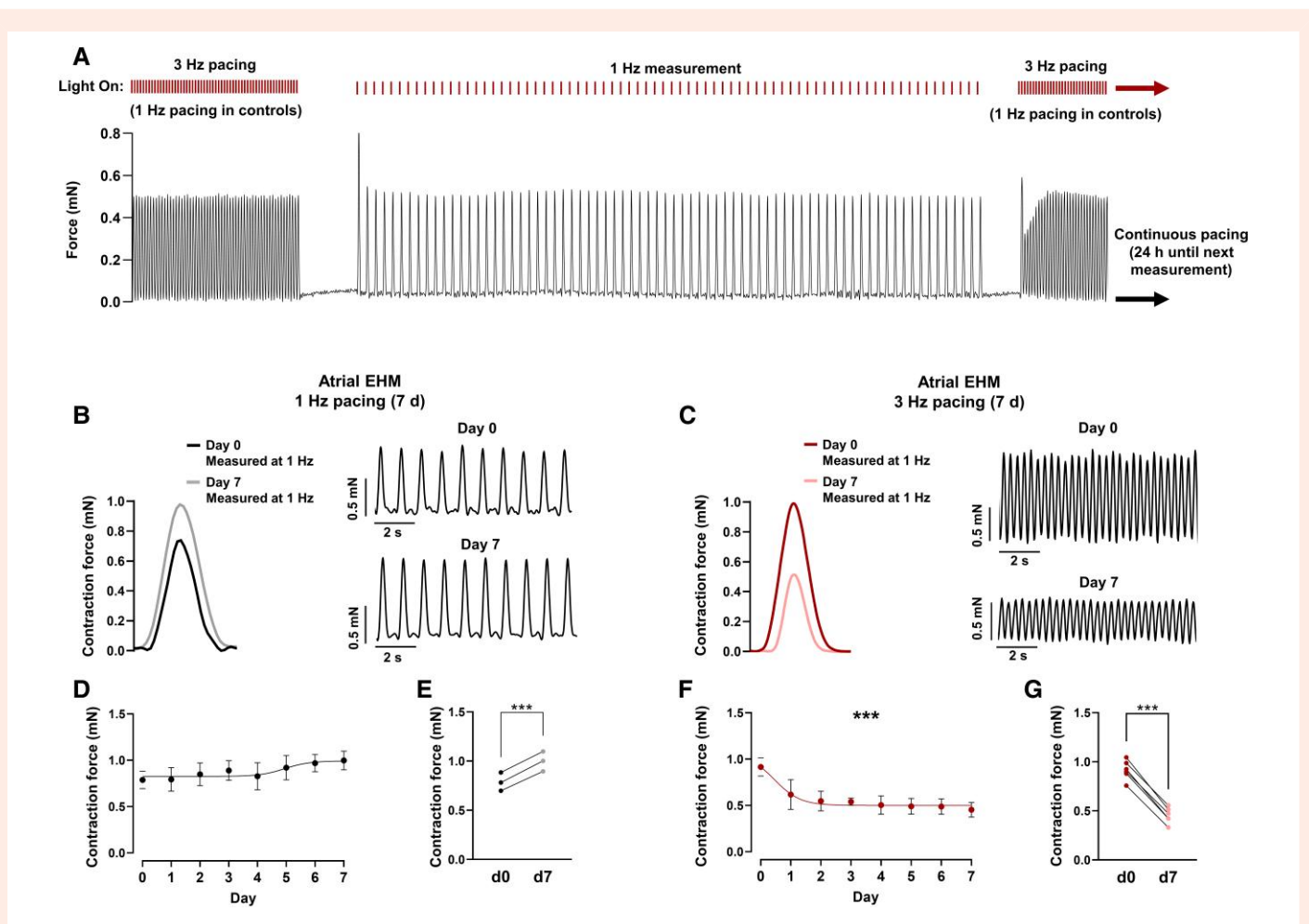


**Figure 7** Prolonged (7-day) TP-induced contractile dysfunction in atrial human engineered myocardium (aEHM). (A) Representative partial trace of aEHM contraction as it is continuously optically stimulated at 3 Hz for 7 days. Contractile measurements were taken every 24 h at a window of 1 Hz pacing, of which a representative example is shown. (B) Representative average contractile signals from aEHM during 7 day 1 Hz optical pacing on day 0 and day 7 (left), representative partial traces of aEHM contraction on day 0 (top right) and day 7 (bottom right) of 1 Hz pacing. (C) Representative average contractile signals from aEHM tissue during 7 day 3 Hz optical pacing on day 0 and day 7 (left), representative partial traces of aEHM contraction on day 0 (top right) and day 7 (bottom right) of 3 Hz pacing. (D) Time course of contractile function of aEHM optically paced for 7 d at 1 Hz ( $n = 3$ ). (E) Change in contractile force after 7 day of optical pacing at 1 Hz. Single point data extracted from (D). (F) Time course of contractile function of aEHM optically paced for 7 day at 3 Hz ( $n = 6$ ). (G) Change in contractile force after 7 day of optical pacing at 3 Hz. Single point data extracted from (F). Data are mean  $\pm$  SEM. \*\*\* $P < 0.001$  vs. 1 Hz using paired Student's *t*-test (E, G) or an extra sum of squares F test to compare fitted sigmoidal curves (D, F).  $n =$  number of EHM.

arrhythmogenic substrate can only be investigated to a very limited extent. Animal models allow for careful control of potential disease-modifying factors and are therefore useful tools for the exploration of mechanistic hypotheses.<sup>6,7</sup> However, especially with respect to cellular electrophysiology and  $\text{Ca}^{2+}$  handling, animal models show substantial differences from the human atrium, which may explain why findings obtained in myocytes from animal models often cannot be reproduced in human atrial myocytes.<sup>8</sup> There is hope that the development of human atrial tissue models based on iPSC-aCM represents a valuable tool to bridge the translational gap between basic arrhythmia research and clinical applications. In fact, a recently issued statement by the US Food and Drug Administration (FDA) emphasized that data from *in vitro* models may be increasingly accepted as pivotal evidence to support clinical trial applications.

In an attempt to promote subtype-directed differentiation, retinoic acid has been shown to regulate the fate specification of atrial vs. ventricular myocytes during cardiac differentiation of human pluripotent stem cells.<sup>11,59,60</sup> Shorter APD is a consistent observation in atrial vs. ventricular iPSC-CM, which is mirrored by our findings.<sup>11,12,60–62</sup> APD<sub>50</sub> of iPSC-aCM are comparable to values

of APD<sub>50</sub> obtained in freshly isolated native human atrial myocytes from patients undergoing open heart surgery.<sup>2,3</sup> Furthermore, aEHM generated from iPSC-aCM are enriched in atrial-specific markers [*NPPA*, *KCNJ3* and *GJA5*, myosin light chain 2A (*MYL2*)] whereas ventricular markers [myosin light chain 2 V (*MYL2*) and *IRX4*] are almost absent (Figure 1).<sup>11</sup> mRNA of atrial-specific ion channels *Kv1.5* (*KCNAS5*) and *Kir3.1* (*KCNJ3*), which mediate the ultra-rapid delayed rectifier  $\text{K}^+$  current  $I_{\text{Kur}}$  and the acetylcholine-activated inward-rectifier  $\text{K}^+$  current  $I_{\text{KACh}}$ , respectively, show higher expression in iPSC-aCM than in iPSC-vCM (see [Supplementary material online, Figure S3](#)).<sup>11</sup> In accordance, agonist-dependent  $I_{\text{KACh}}$  currents can be activated in atrial but not in ventricular iPSC-CM (Figures 1 and 2, [Supplementary material online, Figure S6](#)).<sup>12,14,63</sup> Here we demonstrate that  $I_{\text{KACh}}$  channel properties were comparable to our previously reported  $I_{\text{KACh}}$  properties in native human atrial myocytes with respect to agonist-dependent activation and desensitization (Figure 1, [Supplementary material online, Figure S4](#)). In agreement with previous data reporting a reduced expression of *Kir2.1* (*KCNJ2*) and *Cav1.2* (*CACNA1C*) in atrial samples,<sup>13,64</sup> we found smaller  $I_{\text{K1}}$  and  $I_{\text{CaL}}$  densities in iPSC-aCM (Figure 1). This was not fully recapitulated on

an mRNA expression level with lower *KCNJ2* ( $P < 0.05$ ), but higher *CACNA1C* (not significant; [Supplementary material online, Figure S3](#)).

In order to simulate atrial arrhythmias, multicellular preparations of iPSC-aCM have been investigated in 2D culture dishes<sup>60</sup> and 3D engineered heart tissue constructs.<sup>65</sup> Both models have been shown to be susceptible to various forms of re-entry, which could be terminated by application of  $\text{Na}^+$ -channel blockers flecainide and vernakalant or electrical stimulation. Whereas these investigations represent an important proof-of-concept, they do not take AF-associated remodelling into account. In particular, specific atrial targets such as  $I_{K_{ur}}$  are downregulated in AF<sup>35</sup> whereas others develop in a disease specific manner such as  $I_{K_{ACH,c}}$  which is absent in healthy atria.<sup>24,25,38</sup> Given that changes in ion channel function caused by electrical remodelling and AF persistence represent a major challenge in AF therapy development,<sup>18,19</sup> electrical remodelling needs to be considered when implementing iPSC-aCM-based models of AF.

Electrical *in vivo* TP in animal models of AF can be applied for more than 4 weeks. However, electrical *in vitro* TP of atrial myocytes is only feasible for about 24 h. This limitation results from adverse Faradic reactions including oxidation of electrodes, generation of chlorine and hydroxyl radicals, and formation of hypochlorous acid and chlorate.<sup>22,66</sup> To overcome this caveat, expression of Channelrhodopsin-2, a light-gated ion channel, using lentiviral-mediated transduction has been employed previously to allow long-term stimulation of EHM.<sup>22,62</sup> However, due to strong desensitization properties of Channelrhodopsin-2, this approach does not allow continuous high-frequency stimulation since a recovery period of 15 s is required after 15 s of 3 Hz burst stimulation to allow channel recovery.<sup>22</sup> This intermittent pacing may explain why, in a recent study using this approach, only limited remodelling was achieved in atrial EHM.<sup>62</sup> To circumvent these difficulties and allow for long-term high-frequency pacing we used a novel Channelrhodopsin variant f-Chrimson with faster on/off kinetics and reduced desensitization properties.<sup>26</sup> We generated an iPSC line expressing f-Chrimson using CRISPR/Cas9 genome editing technology to ensure that all atrial cells derived from this line express f-Chrimson. In contrast to lentiviral transduction methods, which have an efficacy of ~25% according to previous publications,<sup>22,62</sup> this approach further reduces the required light intensity to avoid desensitization during high pacing frequencies. Using this approach we were able to continuously apply 3 Hz pacing for 7 days and successfully induce electrical remodelling in aEHM.

Similar to consistent findings in patients with AF and animal models subjected to TP, here we show for the first time that 24-h TP is sufficient to induce electrical remodelling in iPSC-aCM characterized by APD shortening, downregulation of  $I_{CaL}$  and impaired activity of  $I_{K_{ACH}}$ . Interestingly, 24-h TP of iPSC-vCM and vEHM also induced  $I_{CaL}$  downregulation and AP shortening, which is consistent with previous data<sup>52</sup> and points to a ubiquitous mechanism to avoid cellular  $\text{Ca}^{2+}$  overload by limiting  $\text{Ca}^{2+}$  influx. Nevertheless, 24-h TP was not sufficient to induce upregulation of basal inward-rectifier  $\text{K}^+$  current  $I_{K1}$  and hyperpolarization of the RMP. Similarly, previous findings indicated that 24-h TP of isolated dog atrial myocytes led to AP shortening, reduced  $I_{CaL}$  amplitude and remodelling of  $I_{K_{ACH}}$  but without any effect on RMP, indicating unaltered  $I_{K1}$ .<sup>21,38,39</sup> In fact, we observed RMP hyperpolarization in aEHM after 1 week TP, which is likely to be caused by increased  $I_{K1}$ , suggesting that longer periods of tachycardia are necessary for RMP hyperpolarization. This is consistent with our previous findings in atrial myocytes from patients with paroxysmal AF i.e. AF episodes lasting less than 1 week, showing unaltered amplitudes of basal inward-rectifier  $\text{K}^+$  currents<sup>24,33</sup> whereas agonist-dependent  $I_{K_{ACH}}$  was already reduced.

We propose that the possibility to directly study electrical remodelling in human atrial myocytes will enable more rapid and accurate identification of the underlying mechanisms in a human-specific context. In addition, molecular mechanisms of agonist-independent  $I_{K_{ACH}}$  have been investigated in great detail,<sup>24,34,38</sup> but translation into clinically available treatments have so far failed because currently available drug screening assays are based on non-cardiac cell lines or animal models.<sup>24,25,38</sup> None of them completely represents the nature of constitutively active  $I_{K_{ACH}}$ . Furthermore, although reduced  $I_{K_{ACH}}$  current has been detected in animal models of AF,<sup>38,67</sup> downregulation of underlying Kir3.1 and Kir3.4 channel subunits was

absent in animal models.<sup>39</sup> In contrast, expression of Kir3.4 (*KCNJ5*), but not Kir3.1 (*KCNJ3*) mRNA was reduced in aEHM subjected to TP, which is in accordance with findings in AF patients, where protein expression of Kir3.4 is more strongly reduced compared to Kir3.1.<sup>34</sup> These data indicate that reduced expression of  $I_{K_{ACH}}$  channels represents a human-specific mechanism in  $I_{K_{ACH}}$  remodelling. Furthermore, we describe a phosphorylation-dependent downregulation of  $I_{CaL}$  (Figure 3) in the absence of decreased  $\text{Ca}_v1.2$  (*CACNA1C*) expression (Figure 5) which has also been shown in patients with persistent AF.<sup>5,68</sup> In contrast, animal models of AF-associated remodelling predominantly show a transcriptionally mediated reduction of  $\text{Ca}_v1.2$ .<sup>69–71</sup> This indicates another potential human-specific mechanism in response to atrial TP.

Similar to other common cardiovascular diseases, AF is a multifactorial disease with both environmental and genetic factors contributing to pathogenesis. In addition to familial AF, with early onset and clear hereditary patterns,<sup>72</sup> genome-wide association studies (GWAS) have identified a plethora of common variants associated with AF.<sup>73</sup> Most of those variants are located in non-coding regions of the genome with no clear path from gene to disease mechanism. Unravelling the underlying mechanisms will likely require large-scale functional screening assays that are able to reproduce major aspects of atrial electrophysiology and are susceptible to AF-associated electrical remodelling. In addition, it is assumed that genomic variability underlying AF also contributes to the variable responses of patients to antiarrhythmic therapy.<sup>74</sup> Therefore, personalized atrial models based on iPSC-aCM may be useful for predicting patients' individual drug response. Finally, it is presumable that gene variants associated with AF not only increase the susceptibility to AF induction but also facilitate the development of electrical remodelling thereby promoting AF maintenance in certain patients. Our present findings suggest that iPSC-aCM not only represents a valuable tool to study the impact of genetic variants on atrial electrophysiology and drug response, but they can also be employed to study whether certain variants promote or protect from electrical remodelling. Therefore, these models represent an important step towards personalized treatment of AF.

### 4.3 Potential limitations

It is important to be aware that there is no 'perfect' model of AF.<sup>7</sup> The pathophysiology of AF in the individual patient is a complex function of underlying diseases, genetic predisposition and environmental factors. In fact, electrophysiological phenotypes differ from patients with long-term persistent AF,<sup>3,24,25</sup> paroxysmal AF,<sup>2,33,75</sup> postoperative AF<sup>76</sup> or AF in patients with heart failure.<sup>77</sup> Therefore, any model of AF only reproduces certain aspects of this complex phenotype and models need to be chosen based on the research question being asked. Accordingly, it is well known that iPSC-aCM represent a rather immature developmental stage. Immature subcellular structure,  $\text{Ca}^{2+}$ -handling properties and the presence of depolarizing ion currents resulting in spontaneous activity need to be considered when using iPSC-based models.<sup>78–80</sup> In addition, although expression of Kv1.5 channels is significantly higher in iPSC-aCM compared to iPSC-vCM,<sup>11</sup> corresponding  $I_{K_{ur}}$  currents<sup>81</sup> are still small compared to native human atrial CM.<sup>82,83</sup> This may explain why we were not able to detect a prolongation of APD<sub>20</sub> in response to 3-Hz TP, which is supposed to represent an accepted hallmark of AF-associated remodelling caused by  $I_{K_{ur}}$  downregulation.<sup>1,2</sup> Nevertheless, human iPSC-CM present a readily available human model of cardiomyocytes which can be generated on demand in large quantities, making them a promising model to investigate electrophysiological abnormalities in patients.<sup>11</sup>

For technical reasons, high-throughput electrophysiological recordings of  $I_{CaL}$  (Figures 1 and 3) and inward-rectifier potassium currents (Figure 6) were performed at room temperature only.<sup>13</sup> Whereas previously published data render temperature effects on  $I_{K1}$  and  $I_{K_{ACH}}$  unlikely,<sup>33</sup>  $I_{CaL}$  amplitudes are clearly temperature dependent. However, additional experiments performed at 37°C using conventional patch-clamp confirmed our findings of clearly smaller  $I_{CaL}$  amplitude after 24 h electrical TP at 3 Hz compared to pacing at 1 Hz (see [Supplementary material online, Figure S7](#)).

## 5. Conclusions

In this study, we developed a new AF model based on iPSC-aCM and aEHM. We clearly demonstrate that electrical TP of iPSC-aCM and aEHM induces electrophysiological remodelling resembling the situation in patients with persistent AF. In particular, we observed shorter APD, reduced  $I_{Ca,L}$  and  $I_{K,ACh}$  and development of agonist independent constitutively active  $I_{K,ACh}$ .

We furthermore introduced a new iPSC-line expressing fast Channelrhodopsin f-Chrimson. This allowed for novel continuous long-term *in vitro* TP of cardiac tissue in general and of aEHM in particular. Thereby we could demonstrate that various hallmarks of electrical remodelling develop at different time points with APD shortening, abnormal  $I_{Ca,L}$  and  $I_{K,ACh}$  activity being early events whereas RMP hyperpolarization could only be detected after 1 week.

Taken together, we believe that these models represent an important new tool for studying mechanisms underlying AF-associated electrical remodelling in humans and for the development of new patient-tailored antiarrhythmic therapy.

## Supplementary material

Supplementary material is available at *Cardiovascular Research* online.

## Acknowledgements

We are grateful for the excellent technical assistance by Laura Cyganek, Nadine Gotzmann, Yvonne Hintz, Lisa Krebs and Yvonne Wedekind (all Stem Cell Unit, UMG); Yvonne Metz and Johanna Heine (all KSB lab), Stefanie Kestel, Ines Müller and Iris Quentin. The authors thank Maren Dilaj for excellent secretarial help and Dr. Fleur Mason for careful proofreading of the manuscript. Generation of the GMP line LiPSC-GR1.1 (also known as TC1133 or RUCDRi002-A) was supported by the NIH Common Fund Regenerative Medicine Program and reported in *Stem Cell Reports*.<sup>29</sup> The NIH Common Fund and the National Center for Advancing Translational Sciences (NCATS) are joint stewards of the LiPSC-GR1.1 resource. A derivative from a GMP working cell bank of the TC1133-line (Master Cell Bank Lot#: 50-001-21 processed into a working cell bank by Repairon GmbH) was made available to UMG by myriamed GmbH for non-commercial research use. We thank Dr. Tobias Moser and Dr. Ernst Bamberg for providing the f-Chrimson sequence and Dr. Eric Schoger and Dr. Laura Zelarayan for providing help with the generation of the f-Chrimson iPSC-line.

**Conflict of interest:** W.H.Z. is founder and advisor of Repairon GmbH and myriamed GmbH. M.T. is advisor of Repairon GmbH and myriamed GmbH. myriamed GmbH commercializes iPSC-based cell and tissue models for drug discovery. M.Rap. is an employee of Nanion Technologies GmbH. This manuscript was handled by Consulting Editor David Eisner.

## Funding

This work was supported by the Deutsche Forschungsgemeinschaft to N.V. (DFG, VO 1568/3-1, VO 1568/4-1, IRTG1816 project 12, SFB1002 project A13 and under Germany's Excellence Strategy—EXC 2067/1-390729940), to K.S.-B. (STR 1411/7-1), to L.C. [SFB 1002 project S01, MBExC (EXC 2067/1)]; by the DZHK to N.V. (German Center for Cardiovascular Research, 81X4300102, 'DNAfix'), to K.S.-B. (81X4300114) and by the BMBF subproject of the German Network for RASopathy Research (GeNeRARE) to G.K. (01GM1902D). This work was further supported by a scholarship from the Göttingen Promotionskolleg für Medizinstudierende, funded by the Jacob-Henle-Programm and the Else-Kröner-Fresenius-Stiftung to M.Rit. W.H.Z. is supported by DFG SFB 1002 projects C04 and S01, DZHK, BMBF (161L0250A), the Fondation Leducq (20CVD04), and MBExC (EXC 2067/1).

## Data availability

All available data are incorporated into this article and its online supplementary material.

## References

- Nattel S, Heijman J, Zhou L, Dobrev D. Molecular basis of atrial fibrillation pathophysiology and therapy: a translational perspective. *Circ Res* 2020;**127**:51–72.
- Heijman J, Voigt N, Nattel S, Dobrev D. Cellular and molecular electrophysiology of atrial fibrillation initiation, maintenance, and progression. *Circ Res* 2014;**114**:1483–1499.
- Voigt N, Li N, Wang Q, Wang W, Trafford AW, Abu-Taha I, Sun Q, Wieland T, Ravens U, Nattel S, Wehrens XHT, Dobrev D. Enhanced sarcoplasmic reticulum  $Ca^{2+}$  leak and increased  $Na^+Ca^{2+}$  exchanger function underlie delayed afterdepolarizations in patients with chronic atrial fibrillation. *Circulation* 2012;**125**:2059–2070.
- Van Wagoner DR, Pond AL, Lamorgese M, Rossie SS, McCarthy PM, Nerbonne JM. Atrial L-type  $Ca^{2+}$  currents and human atrial fibrillation. *Circ Res* 1999;**85**:428–436.
- Christ T, Boknik P, Wöhrl S, Wettwer E, Graf EM, Bosch RF, Knaut M, Schmitz W, Ravens U, Dobrev D. L-type  $Ca^{2+}$  current downregulation in chronic human atrial fibrillation is associated with increased activity of protein phosphatases. *Circulation* 2004;**110**:2651–2657.
- Schüttler D, Bapat A, Kaab S, Lee K, Tomsits P, Clauss S, Hucker WJ. Animal models of atrial fibrillation. *Circ Res* 2020;**127**:91–110.
- Nishida K, Michael G, Dobrev D, Nattel S. Animal models for atrial fibrillation: clinical insights and scientific opportunities. *Eurpace* 2010;**12**:160–172.
- Liutkute A, Brundel BJ, Voigt N. Not the classical serendipity: does dofetilide treat atrial fibrillation? *Cardiovasc Res* 2022;**118**:1613–1614.
- Brandenburg S, Pawlowitz J, Fakuade FE, Kownatzki-Danger D, Kohl T, Mitronova GY, Scardigli M, Neef J, Schmidt C, Wiedmann F, Pavone FS, Sacconi L, Kutschka I, Sossalla S, Moser T, Voigt N, Lehnart SE. Axial tubule junctions activate atrial  $Ca^{2+}$  release across Species. *Front Physiol* 2018;**9**:1227.
- Zhao Y, Rafatian N, Feric NT, Cox BJ, Aschar-Sobbi R, Wang EY, Aggarwal P, Zhang B, Conant G, Ronaldson-Bouchard K, Pahnke A, Protze S, Lee JH, Davenport Huyer L, Jekic D, Wickeler A, Naguib HE, Keller GM, Vunjak-Novakovic G, Broecker U, Backx PH, Radisic M. A platform for generation of chamber-specific cardiac tissues and disease modeling. *Cell* 2019;**176**:913–927.e18.
- Cyganek L, Tiburcy M, Sekeres K, Gerstenberg K, Bohnenberger H, Lenz C, Henze S, Stauske M, Salinas G, Zimmermann WH, Hasenfuss G, Guan K. Deep phenotyping of human induced pluripotent stem cell-derived atrial and ventricular cardiomyocytes. *JCI Insight* 2018;**3**:e99941.
- Lee JH, Protze SI, Laksman Z, Backx PH, Keller GM. Human pluripotent stem cell-derived atrial and ventricular cardiomyocytes develop from distinct mesoderm populations. *Cell Stem Cell* 2017;**21**:179–194.e4.
- Seibertz F, Rapedius M, Fakuade FE, Tomsits P, Liutkute A, Cyganek L, Becker N, Majumder R, Claß S, Fertig N, Voigt N. A modern automated patch-clamp approach for high throughput electrophysiology recordings in native cardiomyocytes. *Commun Biol* 2022;**5**:969.
- Lemme M, Ulmer BM, Lemoine MD, Zech ATL, Flenner F, Ravens U, Reichenspurner H, Rol-Garcia M, Smith G, Hansen A, Christ T, Eschenhagen T. Atrial-like engineered heart tissue: an *in vitro* model of the human atrium. *Stem Cell Rep* 2018;**11**:1378–1390.
- Stillitano F, Hansen J, Kong CW, Karakikes I, Funck-Brentano C, Geng L, Scott S, Reynier S, Wu M, Valogne Y, Desseaux C, Salem JE, Jeziorowska D, Zahr N, Li R, Iyengar R, Hajjar RJ, Hulot JS. Modeling susceptibility to drug-induced long QT with a panel of subject-specific induced pluripotent stem cells. *Elife* 2017;**6**:e19406.
- Giacomelli E, Bellin M, Sala L, van Meer BJ, Tertoolen LGJ, Orlova VV, Mummery CL. Three-dimensional cardiac microtissues composed of cardiomyocytes and endothelial cells co-differentiated from human pluripotent stem cells. *Development* 2017;**144**:1008–1017.
- Heijman J, Voigt N, Carlsson LG, Dobrev D. Cardiac safety assays. *Curr Opin Pharmacol* 2014;**15**:16–21.
- Duyschaever M, Blauuw Y, Alessie M. Consequences of atrial electrical remodeling for the anti-arrhythmic action of class IC and class III drugs. *Cardiovasc Res* 2005;**67**:69–76.
- Tieleman RG, Van Gelder IC, Bosker HA, Kingma T, Wilde AAM, Kirchhof CJHJ, Bennekens JH, Bracke FAL, Veeger NJGM, Haaksma J, Alessie MA, Crijns HJGM. Does flecainide regain its antiarrhythmic activity after electrical cardioversion of persistent atrial fibrillation? *Heart Rhythm* 2005;**2**:223–230.
- Luo X, Pan Z, Shan H, Xiao J, Sun X, Wang N, Lin H, Xiao L, Maguy A, Qi X-Y, Li Y, Gao X, Dong D, Zhang Y, Bai Y, Ai J, Sun L, Lu H, Luo X-Y, Wang Z, Lu Y, Yang B, Nattel S. MicroRNA-26 governs profibrillatory inward-rectifier potassium current changes in atrial fibrillation. *J Clin Invest* 2013;**123**:1939–1951.
- Qi XY, Yeh YH, Xiao L, Burstein B, Maguy A, Chartier D, Villeneuve LR, Brundel BJM, Dobrev D, Nattel S. Cellular signaling underlying atrial tachycardia remodeling of L-type calcium current. *Circ Res* 2008;**103**:845–854.
- Lemme M, Braren I, Prondzynski M, Akeshirlioglu B, Ulmer BM, Schulze ML, Ismaili D, Meyer C, Hansen A, Christ T, Lemoine MD, Eschenhagen T. Chronic intermittent tachypacing by an optogenetic approach induces arrhythmia vulnerability in human engineered heart tissue. *Cardiovasc Res* 2020;**116**:1487–1499.
- Tiburcy M, Hudson JE, Balfanz P, Schlick S, Meyer T, Liao MLC, Levent E, Raad F, Zeidler S, Wingender E, Riegler J, Wang M, Gold JD, Kehat I, Wettwer E, Ravens U, Dierckx P, Van LL, Goumans MJ, Khadjeh S, Toischer K, Hasenfuss G, Couture LA, Unger A, Linke WA, Araki T, Neel B, Keller G, Gepstein L, Wu JC, Zimmermann WH. Defined engineered human

- myocardium with advanced maturation for applications in heart failure modeling and repair. *Circulation* 2017;**135**:1832–1847.
24. Voigt N, Friedrich A, Bock M, Wettwer E, Christ T, Knaut M, Strasser RH, Ravens U, Dobrev D. Differential phosphorylation-dependent regulation of constitutively active and muscarinic receptor-activated  $I_{K_{ACH}}$  channels in patients with chronic atrial fibrillation. *Cardiovasc Res* 2007;**74**:426–437.
  25. Dobrev D, Friedrich A, Voigt N, Jost N, Wettwer E, Christ T, Knaut M, Ravens U. The G protein-gated potassium current  $I_{K_{ACH}}$  is constitutively active in patients with chronic atrial fibrillation. *Circulation* 2005;**112**:3697–3706.
  26. Mager T, Lopez de la Morena D, Senn V, Schlotte J, Derrico A, Feldbauer K, Wrobel C, Jung S, Bodensiek K, Rankovic V, Browne L, Huet A, Jüttner J, Wood PG, Letzkus JJ, Moser T, Bamberg E. High frequency neural spiking and auditory signaling by ultrafast red-shifted optogenetics. *Nat Commun* 2018;**9**:1750.
  27. Kleinsorge M, Cyganek L. Subtype-Directed differentiation of human iPSCs into atrial and ventricular cardiomyocytes. *STAR Protoc* 2020;**1**:100026.
  28. Schoger E, Argyriou L, Zimmermann WH, Cyganek L, Zelarayan LC. Generation of homozygous CRISPRa human induced pluripotent stem cell (hiPSC) lines for sustained endogenous gene activation. *Stem Cell Res* 2020;**48**:101944. doi: 10.1016/j.scr.2020.101944.
  29. Baghbaderani BA, Tian X, Neo BH, Burkall A, Dimezzo T, Sierra G, Zeng X, Warren K, Kovarick DP, Fellner T, Rao MS. CGMP-manufactured human induced pluripotent stem cells are available for pre-clinical and clinical applications. *Stem Cell Rep* 2015;**5**:647–659.
  30. Tiburcy M, Meyer T, Liaw NY, Zimmermann WH. Generation of engineered human myocardium in a multi-well format. *STAR Protoc* 2020;**1**:100032.
  31. Kensah G, Roa Lara A, Dahlmann J, Zweigerdt R, Schwanke K, Hegermann J, Skvorc D, Gawol A, Azizian A, Wagner S, Maier LS, Krause A, Dräger G, Ochs M, Haverich A, Gruh I, Martin U. Murine and human pluripotent stem cell-derived cardiac bodies form contractile myocardial tissue in vitro. *Eur Heart J* 2013;**34**:1134–1146.
  32. Seibert F, Reynolds M, Voigt N. Single-cell optical action potential measurement in human induced pluripotent stem cell-derived cardiomyocytes. *J Vis Exp* 2020;**2020**:e61890.
  33. Voigt N, Trausch A, Knaut M, Matschke K, Varró A, Van Wagoner DR, Nattel S, Ravens U, Dobrev D. Left-to-right atrial inward rectifier potassium current gradients in patients with paroxysmal versus chronic atrial fibrillation. *Circ Arrhythmia Electrophysiol* 2010;**3**:472–480.
  34. Voigt N, Heijman J, Trausch A, Mintert-Jancke E, Pott L, Ravens U, Dobrev D. Impaired  $Na^+$ -dependent regulation of acetylcholine-activated inward-rectifier  $K^+$  current modulates action potential rate dependence in patients with chronic atrial fibrillation. *J Mol Cell Cardiol* 2013;**61**:142–152.
  35. Wettwer E, Hála O, Christ T, Heubach JF, Dobrev D, Knaut M, Varró A, Ravens U. Role of  $I_{K_{ur}}$  in controlling action potential shape and contractility in the human atrium: influence of chronic atrial fibrillation. *Circulation* 2004;**110**:2299–2306.
  36. Tiburcy M, Didié M, Boy O, Christalla P, Döker S, Naito H, Karikkineth BC, El-Armouche A, Grimm M, Nose M, Eschenhagen T, Ziesenker A, Katschinski DM, Hamdani N, Linke WA, Yin X, Mayr M, Zimmermann WH. Terminal differentiation, advanced organotypic maturation, and modeling of hypertrophic growth in engineered heart tissue. *Circ Res* 2011;**109**:1105–1114.
  37. Calloe K, Goodrow R, Olesen SP, Antzelevitch C, Cordeiro JM. Tissue-specific effects of acetylcholine in the canine heart. *Am J Physiol Hear Circ Physiol* 2013;**305**:H66–H75.
  38. Makary S, Voigt N, Maguy A, Wakili R, Nishida K, Harada M, Dobrev D, Nattel S. Differential protein kinase c isoform regulation and increased constitutive activity of acetylcholine-regulated potassium channels in atrial remodeling. *Circ Res* 2011;**109**:1031–1043.
  39. Voigt N, Maguy A, Yeh YH, Qi X, Ravens U, Dobrev D, Nattel S. Changes in  $I_{K_{ACH}}$  single-channel activity with atrial tachycardia remodeling in canine atrial cardiomyocytes. *Cardiovasc Res* 2008;**77**:35–43.
  40. Levay M, Krobert KA, Wittig K, Voigt N, Bermudez M, Wolber G, Dobrev D, Levy FO, Wieland T. NSC23766, A widely used inhibitor of rac1 activation, additionally acts as a competitive antagonist at muscarinic acetylcholine receptors. *J Pharmacol Exp Ther* 2013;**347**:69–79.
  41. Wang Z, Yue L, White M, Pelletier G, Nattel S. Differential distribution of inward rectifier potassium channel transcripts in human atrium versus ventricle. *Circulation* 1998;**98**:2422–2428.
  42. Varró A, Nánási PP, Lathrop DA. Potassium currents in isolated human atrial and ventricular cardiocytes. *Acta Physiol Scand* 1993;**149**:133–142.
  43. Jung P, Seibert F, Fakuade FE, Ignatyeva N, Sampathkumar S, Ritter M, Li H, Mason FE, Ebert A, Voigt N. Increased cytosolic calcium buffering contributes to a cellular arrhythmogenic substrate in iPSC-cardiomyocytes from patients with dilated cardiomyopathy. *Basic Res Cardiol* 2022;**117**:5.
  44. Heijman J, Kirchner D, Kunze F, Chrétien EM, Michel-Reher MB, Voigt N, Knaut M, Michel MC, Ravens U, Dobrev D. Muscarinic type-1 receptors contribute to  $I_{K_{ACH}}$  in human atrial cardiomyocytes and are upregulated in patients with chronic atrial fibrillation. *Int J Cardiol* 2018;**255**:61–68.
  45. Hindricks G, Potpara T, Dagres N, Bax JJ, Boriani G, Dan GA, Fauchier L, Kalman JM, Lane DA, Lettino M, Pinto FJ, Thomas GN, Valgimigli M, Kirchhof P, Kühne M, Aboyan V, Ahlsson A, Balsam P, Bauersachs J, Benussi S, Brandes A, Braunschweig F, Camm AJ, Capodanno D, Casadei B, Conen D, Crijs HJ, Delgado V, Dobrev D, Drexler H, Eckardt L, Fitzsimons D, Folliquet T, Gale CP, Gorenek B, Hauesler KG, Heidbüchel H, Iung B, Katus HA, Kotecha D, Landmesser U, Leclercq C, Lewis BS, Mascherbauer J, Merino JL, Merkely B, Mont L, Mueller C, Nagy K V, Oldgren J, Pavlović N, Pedretti RFE, Petersen SE, Piccini JP, Popescu BA, Pürerfellner H, Richter DJ, Roffi M, Rubboli A, Scherr D, Schnabel RB, Simpson IA, Shlyakhto E, Sinner MF, Steffel J, Sousa-Uva M, Suwalski P, Svetlosak M, Touyz RM, Arbelo E, Blomström-Lundqvist C, Castella M, Dilaveris PE, Filippatos G, Lebeau JP, Lip GYH, Neil Thomas G, Van Gelder IC, Watkins CL. 2020 ESC guidelines for the diagnosis and management of atrial fibrillation developed in collaboration with the European association for cardio-thoracic surgery (EACTS). *Eur Heart J* 2021;**42**:373–498.
  46. Thomas D, Christ T, Fabritz L, Goette A, Hammwöhner M, Heijman J, Kocksämper J, Linz D, Odening KE, Schweizer PA, Wakili R, Voigt N. German Cardiac Society Working Group on cellular electrophysiology state-of-the-art paper: impact of molecular mechanisms on clinical arrhythmia management. *Clin Res Cardiol* 2019;**108**:577–599.
  47. Wijffels MC, Kirchhof CJ, Dorland R, Allesie MA. Atrial fibrillation begets atrial fibrillation: a study in awake chronically instrumented goats. *Circulation* 1995;**92**:1954–1968.
  48. Schmidt C, Wiedmann F, Voigt N, Zhou XB, Heijman J, Lang S, Albert V, Kallenberger S, Ruhparwar A, Szabó G, Kallenbach K, Karck M, Borggreve M, Biliczki P, Ehrlich JR, Baczkó I, Lugenbiel P, Schweizer PA, Donner BC, Katus HA, Dobrev D, Thomas D. Upregulation of  $K2P3.1 K^+$  current causes action potential shortening in patients with chronic atrial fibrillation. *Circulation* 2015;**132**:82–92.
  49. Heijman J, Erfanian Abdoust P, Voigt N, Nattel S, Dobrev D. Computational models of atrial cellular electrophysiology and calcium handling, and their role in atrial fibrillation. *J Physiol* 2016;**594**:537–553.
  50. Cardin S, Libby E, Pelletier P, Le Bouter S, Shiroshita-Takeshita A, Le Meur N, Léger J, Demolombe S, Ponton A, Glass L, Nattel S. Contrasting gene expression profiles in two canine models of atrial fibrillation. *Circ Res* 2007;**100**:425–433.
  51. Lenaerts I, Driesen RB, Blanco NH, Holemans P, Heidbüchel H, Janssens S, Balligand JL, Sipido KR, Willems R. Role of nitric oxide and oxidative stress in a sheep model of persistent atrial fibrillation. *Europace* 2013;**15**:754–760.
  52. Lenaerts I, Bito V, Heinzl FR, Driesen RB, Holemans P, D'Hooge J, Heidbüchel H, Sipido KR, Willems R. Ultrastructural and functional remodeling of the coupling between  $Ca^{2+}$  influx and sarcoplasmic reticulum  $Ca^{2+}$  release in right atrial myocytes from experimental persistent atrial fibrillation. *Circ Res* 2009;**105**:876–885.
  53. Greiser M, Kerfant BG, Williams GSB, Voigt N, Harks E, Dibb KM, Giese A, Meszaros J, Verheule S, Ravens U, Allesie MA, Gammie JS, van der Velden J, Lederer WJ, Dobrev D, Schotten U. Tachycardia-induced silencing of subcellular  $Ca^{2+}$  signaling in atrial myocytes. *J Clin Invest* 2014;**124**:4759–4772.
  54. Schmidt C, Wiedmann F, Tristram F, Anand P, Wenzel W, Lugenbiel P, Schweizer PA, Katus HA, Thomas D. Cardiac expression and atrial fibrillation-associated remodeling of  $K2P2.1 (TREK-1) K^+$  channels in a porcine model. *Life Sci* 2014;**97**:107–115.
  55. Voigt N, Dobrev D. Atrial-Selective potassium channel blockers. *Card Electrophysiol Clin* 2016;**8**:411–421.
  56. Bingen BO, Askar SFA, Neshati Z, Feola I, Panfilov AV, de Vries AA, Pijnappels DA. Constitutively active acetylcholine-dependent potassium current increases atrial defibrillation threshold by favoring post-shock Re-initiation. *Sci Rep* 2015;**5**:15187.
  57. Yoo S, Pfenninger A, Hoffman J, Zhang W, Ng J, Burrell A, Johnson DA, Gussak G, Waugh T, Bull S, Benefield B, Knight BP, Passman R, Wasserstrom JA, Aistrup GL, Arora R. Attenuation of oxidative injury with targeted expression of NADPH oxidase 2 short hairpin RNA prevents onset and maintenance of electrical remodeling in the canine atrium. *Circulation* 2020;**142**:1261–1278.
  58. Mason FE, Pronto JRD, Alhussini K, Maack C, Voigt N. Cellular and mitochondrial mechanisms of atrial fibrillation. *Basic Res Cardiol* 2020;**115**:72.
  59. Zhang Q, Jiang J, Han P, Yuan Q, Zhang J, Zhang X, Xu Y, Cao H, Meng Q, Chen L, Tian T, Wang X, Li P, Hescheler J, Ji G, Ma Y. Direct differentiation of atrial and ventricular myocytes from human embryonic stem cells by alternating retinoid signals. *Cell Res* 2011;**21**:579–587.
  60. Laksman Z, Wauchop M, Lin E, Protze S, Lee J, Yang W, Izaddoustdar F, Shafaattalab S, Gepstein L, Tibbits GF, Keller G, Backx PH. Modeling atrial fibrillation using human embryonic stem cell-derived atrial tissue. *Sci Rep* 2017;**7**:5268.
  61. Devalia HD, Schwach V, Ford JW, Milnes JT, El-Haou S, Jackson C, Gkatzis K, Elliott DA, Chuva de Sousa Lopes SM, Mummery CL, Verkerk AO, Passier R. Atrial-like cardiomyocytes from human pluripotent stem cells are a robust preclinical model for assessing atrial-selective pharmacology. *EMBO Mol Med* 2015;**7**:394–410.
  62. Lemoine MD, Lemme M, Ulmer BM, Braren I, Krasemann S, Hansen A, Kirchhof P, Meyer C, Eschenhagen T, Christ T. Intermittent optogenetic tachypacing of atrial engineered heart tissue induces only limited electrical remodeling. *J Cardiovasc Pharmacol* 2020;**77**:291–299.
  63. Veerman CC, Mengarelli I, Koopman CD, Wilders R, van Amersfoort SC, Bakker D, Wolswinkel R, Hababa M, de Boer TP, Guan K, Milnes J, Lodder EM, Bakkers J, Verkerk AO, Bezzina CR. Genetic variation in  $GNB5$  causes bradycardia by augmenting the cholinergic response via increased acetylcholine-activated potassium current ( $I_{K_{ACH}}$ ). *DMM Dis Model Mech* 2019;**12**:dmm037994.
  64. Gaborit N, Le BS, Szuts V, Varro A, Escande D, Nattel S, Demolombe S. Regional and tissue specific transcript signatures of ion channel genes in the non-diseased human heart. *J Physiol* 2007;**582**:675–693.
  65. Goldfracht I, Protze S, Shiti A, Setter N, Gruber A, Shaheen N, Nartiss Y, Keller G, Gepstein L. Generating ring-shaped engineered heart tissues from ventricular and atrial human pluripotent stem cell-derived cardiomyocytes. *Nat Commun* 2020;**11**:75.
  66. Zhang C, He D, Ma J, Tang W, Waite TD. Faradaic reactions in capacitive deionization (CDI) —problems and possibilities: a review. *Water Res* 2018;**128**:314–330.
  67. Ehrlich JR, Cha TJ, Zhang L, Chartier D, Villeneuve L, Hébert TE, Nattel S. Characterization of a hyperpolarization-activated time-dependent potassium current in canine cardiomyocytes from pulmonary vein myocardial sleeves and left atrium. *J Physiol* 2004;**557**:583–597.

68. Grammatika Pavlidou N, Dobrev S, Beneke K, Reinhardt F, Pecha S, Jacquet E, Abu-Taha IH, Schmidt C, Voigt N, Kamler M, Schnabel RB, Baczkó I, Garnier A, Reichenspurner H, Nikolaev VO, Dobrev D, Molina CE. Phosphodiesterase 8 governs cAMP/PKA-dependent reduction of L-type calcium current in human atrial fibrillation: a novel arrhythmogenic mechanism. *Eur Heart J* 2023;**44**:2483–2494.
69. Yue L, Feng J, Gaspo R, Li GR, Wang Z, Nattel S. Ionic remodeling underlying action potential changes in a canine model of atrial fibrillation. *Circ Res* 1997;**81**:512–525.
70. Bosch RF, Scherer CR, Rüb N, Wöhrl S, Steinmeyer K, Haase H, Busch AE, Seipel L, Kühlkamp V. Molecular mechanisms of early electrical remodeling: transcriptional downregulation of ion channel subunits reduces I(Ca, L) and I(to) in rapid atrial pacing in rabbits. *J Am Coll Cardiol* 2003;**41**:858–869.
71. Gaspo R, Sun H, Fareh S, Levi M, Yue L, Allen BG, Hebert TE, Nattel S. Dihydropyridine and beta adrenergic receptor binding in dogs with tachycardia-induced atrial fibrillation. *Cardiovasc Res* 1999;**42**:434–442.
72. Benzonzi P, Campostrini G, Landi S, Bertini V, Marchina E, Iascone M, Ahlberg G, Olesen MS, Crescini E, Mora C, Bisleri G, Muneretto C, Ronca R, Presta M, Poliani PL, Piovani G, Verardi R, Di Pasquale E, Consiglio A, Raya A, Torre E, Lodrini AM, Milanese R, Rocchetti M, Baruscotti M, DiFrancesco D, Memo M, Barbuti A, Dell’Era P. Human iPSC modelling of a familial form of atrial fibrillation reveals a gain of function of  $I_f$  and  $I_{CaL}$  in patient-derived cardiomyocytes. *Cardiovasc Res* 2020;**116**:1147–1160.
73. Roselli C, Rienstra M, Ellinor PT. Genetics of atrial fibrillation in 2020. *Circ Res* 2020;**127**:21–33.
74. Kany S, Reissmann B, Metzner A, Kirchhof P, Darbar D, Schnabel RB. Genetics of atrial fibrillation-practical applications for clinical management: if not now, when and how? *Cardiovasc Res* 2021;**117**:1718–1731.
75. Voigt N, Heijman J, Wang Q, Chiang DY, Li N, Karck M, Wehrens XHT, Nattel S, Dobrev D. Cellular and molecular mechanisms of atrial arrhythmogenesis in patients with paroxysmal atrial fibrillation. *Circulation* 2014;**129**:145–156.
76. Fakuade FE, Steckmeister V, Seibert F, Gronwald J, Kestel S, Menzel J, Pronto JRD, Taha K, Haghghi F, Kensah G, Pearman CM, Wiedmann F, Teske AJ, Schmidt C, Dibb KM, El-Essawi A, Danner BC, Baraki H, Schwappach B, Kutschka I, Mason FE, Voigt N. Altered atrial cytosolic calcium handling contributes to the development of postoperative atrial fibrillation. *Cardiovasc Res* 2021;**117**:1790–1801.
77. Schmidt C, Wiedmann F, Zhou XB, Heijman J, Voigt N, Ratte A, Lang S, Kallenberger SM, Campana C, Weymann A, De SR, Szabo G, Ruhparwar A, Kallenbach K, Karck M, Ehrlich JR, Baczkó I, Borggreve M, Ravens U, Dobrev D, Katus HA, Thomas D. Inverse remodelling of K2P3.1  $K^+$  channel expression and action potential duration in left ventricular dysfunction and atrial fibrillation: implications for patient-specific antiarrhythmic drug therapy. *Eur Heart J* 2017;**38**:1764–1774.
78. Casini S, Verkerk AO, Remme CA. Human iPSC-derived cardiomyocytes for investigation of disease mechanisms and therapeutic strategies in inherited arrhythmia syndromes: strengths and limitations. *Cardiovasc Drugs Ther* 2017;**31**:325–344.
79. Lee YK, Ng KM, Lai WH, Chan YC, Lau YM, Lian Q, Tse HF, Siu CW. Calcium homeostasis in human induced pluripotent stem cell-derived cardiomyocytes. *Stem Cell Rev Rep* 2011;**7**:976–986.
80. Rao C, Prodromakis T, Kolker L, Chaudhry UAR, Trantidou T, Sridhar A, Weekes C, Camelliti P, Harding SE, Darzi A, Yacoub MH, Athanasiou T, Terracciano CM. The effect of microgrooved culture substrates on calcium cycling of cardiac myocytes derived from human induced pluripotent stem cells. *Biomaterials* 2013;**34**:2399–2411.
81. Hilderink S, Devalla HD, Bosch L, Wilders R, Verkerk AO. Ultrarapid delayed rectifier  $K(+) channelopathies$  in human induced pluripotent stem cell-derived cardiomyocytes. *Front cell Dev Biol* 2020;**8**:536.
82. Ford J, Milnes J, Wettwer E, Christ T, Rogers M, Sutton K, Madge D, Virag L, Jost N, Horvath Z, Matschke K, Varro A, Ravens U. Human electrophysiological and pharmacological properties of XEN-D0101: a novel atrial-selective  $Kv1.5/IKur$  inhibitor. *J Cardiovasc Pharmacol* 2013;**61**:408–415.
83. Christ T, Wettwer E, Voigt N, Hála O, Radicke S, Matschke K, Várro A, Dobrev D, Ravens U. Pathology-specific effects of the  $I_{Kur}/I_{to}/I_{K}$ , ACh blocker AVE0118 on ion channels in human chronic atrial fibrillation. *Br J Pharmacol* 2008;**154**:1619–1630.

## Translational perspective

Atrial fibrillation (AF) begets AF through electrical remodelling. Robust human-centric atrial models of AF-associated remodelling are limited. Through tachypacing of atrial subtype-specific induced pluripotent stem cell-derived cardiomyocytes and engineered human myocardium, we provide novel 2D and 3D *in vitro* models that replicate the hallmarks of classical AF-associated electrical remodelling. Optogenetic pacing uniquely enables continuous long-term tachypacing to investigate the time dependence of AF evolution, analogous to the clinical progression of paroxysmal to permanent AF. These models can be implemented in high-throughput screening platforms to facilitate human-centric, atrial-specific development of antiarrhythmic therapies.